Multiphase semiclassical approximation of an electron in a one-dimensional crystalline lattice

I. Homogeneous problems; vanishing exterior potentials.

Laurent Gosse and Peter A. Markowich

Istituto per le Applicazioni del Calcolo; Sezione di Bari
via G. Amendola, 122/I - 70126 BARI, ITALY.
and
Institüt für Mathematik; University of Vienna
Boltzmanngasse, 9 - A-1090 VIENNA, AUSTRIA.

E-mail: l.gosse@area.ba.cnr.it, Peter.Markowich@univie.ac.at

We present a computational approach for the WKB approximation of the wave function of an electron moving in a periodic one-dimensional crystal lattice. We derive a nonstrictly hyperbolic system for the phase and the intensity where the flux functions originate from the Bloch spectrum of the Schrödinger operator. Relying on the framework of the multibranch entropy solutions introduced by Brenier and Corrias, we compute efficiently multiphase solutions using well adapted and simple numerical schemes. In this first part we present computational results for vanishing exterior potentials which demonstrate the effectiveness of the proposed method.

1. INTRODUCTION

This article is the first part of a numerical study of semiclassical approximation of the motion of electrons in short-scale periodic potentials. This phenomenon is quantum mechanical and we shall represent particles as wave packets with localized wave numbers κ. Then if such a wave packet spreads over many lattice periods, the wave number can be considered constant and the dynamics are ruled by the energy bands. This is of common use in solid-state physics, [3].

More precisely, we start from the Schrödinger equation in one space dimension,

$$i\hbar\partial_t\psi + \frac{\hbar^2}{2m}\partial_{xx}\psi = eV(x)\psi, \qquad x \in \mathbb{R} \tag{1}$$

with $\hbar$ the Planck's constant, m and e the electronic mass and charge and $V \in \mathbb{R}$ the periodic potential modeling the interaction with a lattice of ionic cores in one space dimension ($x \in \mathbb{R}$). We first change to "atomic units" for which $\hbar = m = e = 1$. Then we introduce the dimensionless parameter ε as the microscopic-macroscopic ratio; we assume it small and track wave packets with a spatial spreading of the order of $1/\varepsilon$. We recast (1) in macroscopic variables $x \mapsto x/\varepsilon$, $t \mapsto t/\varepsilon$ (*i.e.* we study $O(\varepsilon)$-wavelength solutions) and a scaled problem arises

$$i\varepsilon\partial_t\psi + \frac{\varepsilon^2}{2}\partial_{xx}\psi = V\left(\frac{x}{\varepsilon}\right)\psi, \qquad V(x+2\pi) = V(x), \tag{2}$$

for which the limit $\varepsilon \to 0$ is of special interest. We assumed the period to be 2π on the atomic lengthscale for the sake of simplicity only.

From the mathematical point of view, the asymptotics of (2) correspond to a combined semiclassical and homogenization limit. Rigorous theorems in this direction have been proven in the last decade by the authors of [23, 39, 43, 46]. Wigner transforms of the wave function ψ were extensively used, ("$\bar{\cdot}$" stands for complex conjugation)

$$W(t,x,\xi) = \int_{\mathbb{R}} \psi\left(t, x + \frac{\varepsilon y}{2}\right)\bar{\psi}\left(t, x - \frac{\varepsilon y}{2}\right)\exp(i\xi y).dy, \qquad \xi \in \mathbb{R}.$$

In fact, in order to take full advantage of the periodic structure of (1), the right object has been found to be the so-called Wigner series which reads

$$w(t,x,\kappa) = \sum_{j\in\mathbb{Z}} \psi(t, x+\varepsilon j\pi)\bar{\psi}(t, x-\varepsilon j\pi)\exp(-2\pi i\kappa j), \qquad \kappa \in B, \tag{3}$$

and from which one can deduce for instance the electron's position density:

$$\rho(t,x) = \int_B w(t,x,\kappa)\frac{d\kappa}{|B|}, \qquad B \text{ the first Brillouin zone.}$$

A summary of these results will be presented in §2.3. Before going further, some classical definitions are recalled in order to facilitate the understanding of this paper in terms of the existing literature:

- The Bravais lattice for (1), (2) is $\Gamma = 2\pi\mathbb{Z}$; its primitive cell is $]0, 2\pi[$.
- The reciprocal lattice Γ' is the set of wave numbers κ for which plane waves $\exp(i\kappa x)$ have the same periodicity as the potential V; *i.e.* $\Gamma' = \mathbb{Z}$.
- The first Brillouin zone B is the Wigner-Seitz cell of the dual lattice Γ' made of all κ closer to zero than to any other dual lattice point; $B =]-\frac{1}{2}, \frac{1}{2}[$.

Then, by means of (3), one passes from (2) as $\varepsilon \to 0$ to a kinetic equation for a density $f \simeq w$ which is solution of the transport equation:

$$\partial_t f(t,x,\kappa) + E_n'(\kappa)\partial_x f(t,x,\kappa) = 0, \qquad f \geq 0. \tag{4}$$

The set of all functions $E_n(\kappa)$ corresponds to the band structure of (2) whose derivation will be presented in details in §2.2. From these considerations, one could deduce that this "Wigner approach" also indicates a feasable route towards computational algorithms. Indeed, upon taking κ-moments of (4), a system of conservation laws can be written when assuming that $f(t,x,\kappa) = \sum_\ell \rho_\ell(t,x)\delta(\kappa - p_\ell(t,x))$, which means that particles of mass/velocity ρ_ℓ/p_ℓ are tracked in phase space while moving according to the Hamiltonian $E_n(p)$. However, these weakly hyperbolic systems turn out to be rather delicate to simulate [19, 33, 45] since even for the simplest case $\ell \equiv 1$ (the so-called monokinetic density), one faces the pressureless gas problem admitting measure-valued solutions; see [9, 13] and references therein.

An alternative strategy can be proposed relying on classical WKB expansions, see [35] and the original references in [14]. Considerations of this nature usually lead to simpler systems made of a Hamilton-Jacobi equation for the phase of the wave function coupled to a continuity equation for its intensity. However, at this level, the difficulty lies more in finding a way to elicit a correct solution: clearly the framework of viscosity solutions [18, 22, 28] doesn't fit since the entropy conditions destroy the folds generally appearing in phase space. It has been recently shown that when the number of these folds is finite, there exists a way to reconstruct exactly the "geometric solution" , [1, 11, 32] by solving a much less singular moments system. Roughly speaking, it consists in solving (4) with the smoother kinetic density $f(t,x,\kappa) = \sum_\ell (-1)^{\ell-1} H(p_\ell(t,x) - \kappa)$, H the Heaviside function, following [12] as will be developed in §2.4 (the cases $\ell = 1, 2$ have been treated in [11, 40, 41]). This technique has been investigated numerically in [27, 29, 45]; it somewhat takes for granted WKB expansions and then treats them in such a way they render the Correspondence Principle between quantum and classical mechanics. For other methods, we refer the reader to [5, 19, 34, 47]. We stress that, besides a possibly lower computational cost, a semiclassical simulation presents two advantages when compared to a direct simulation of the wave function satisfying (1): it naturally reveals the band and caustic structures.

When carrying out the WKB asymptotics in §2.1 in the spirit of [30], an essential point lies in computing efficiently the Bloch spectrum of the Hamiltonian operator $\mathcal{H}(x, i\partial_x) = -\frac{1}{2}\partial_{xx} + V(x)$. This constitutes one of the main numerical difficulties as it amounts to solving an eigenvalue problem for a Sturm-Liouville equation, [50]. We propose in §2.2 a way around it avoiding semiclassical quantization, [35, 15, 17], but using spectral techniques. Finally, §3–4 are devoted to the study of practical examples including the Mathieu's equation and the Kronig-Penney model, [37]. Numerical computations making use of the so-called parabolic band approximation, [3, 44] for moderate wave numbers and a Fourier representation of the bands when considering the whole Brillouin zone are presented. The most classical approach is of course ray-tracing in phase space; however, its accuracy can sometimes be really low when compared to Eulerian methods, [5, 47]. We also present preliminary numerical comparisons between a direct Fourier simulation of (2) and a multiphase WKB approximation relying on the aforementioned K-branch solutions. In an Appendix, we comment on the connection with effective Hamiltonians obtained when homogenizing Hamilton-Jacobi equations in the sense of [38].

We close this introduction mentioning that in a forthcoming paper (Part II of this work), we shall report on computations with nontrivial exterior potentials; that is to say, approximation for small values of ε of

$$i\varepsilon\partial_t\psi + \frac{\varepsilon^2}{2}\partial_{xx}\psi = \left(V\left(\frac{x}{\varepsilon}\right) + V_e(x)\right)\psi, \tag{5}$$

instead of (2) in case $V_e \in \mathbb{R}$ is smooth. A concrete example is Coulomb interaction; first considerations on this more delicate problem are stated in §5.

2. WKB METHOD IN ONE SPACE DIMENSION

We are concerned with highly oscillating wave-packet solutions of the Cauchy problem for the following one-dimensional Schrödinger equation:

$$i\varepsilon\partial_t\psi + \frac{\varepsilon^2}{2}\partial_{xx}\psi = \left(V\left(\frac{x}{\varepsilon}\right) + V_e(x)\right)\psi, \qquad \varepsilon \to 0, \tag{6}$$

where V is 2π-periodic and V_e is smooth. Generally, one is tempted to describe these solutions by means of plane waves of the form $\psi(t,x) = A(t,x)\exp(i\varphi(t,x)/\varepsilon)$ for A and φ being possibly multivalued; plugging this ansatz into (6) leads to a relation between the wave's phase φ and its amplitude A:

$$-A\left(\partial_t\varphi + \frac{(\partial_x\varphi)^2}{2} + V\left(\frac{x}{\varepsilon}\right) + V_e(x)\right) + \frac{i\varepsilon}{2}\Big(2\partial_t A + A\partial_{xx}\varphi + 2\partial_x A\,\partial_x\varphi\Big) + \frac{\varepsilon^2}{2}\partial_{xx}A = 0.$$

Splitting this equation into real and imaginary parts yields:

$$\partial_t\varphi + \frac{(\partial_x\varphi)^2}{2} + V\left(\frac{x}{\varepsilon}\right) + V_e(x) = \frac{\varepsilon^2}{2A}\partial_{xx}A, \qquad \partial_t(A^2) + \partial_x(A^2\ \partial_x\varphi) = 0. \tag{7}$$

Moreover, neglecting the term $\varepsilon^2\partial_{xx}A/2A$ leads to the weakly coupled system:

$$\partial_t\varphi + \frac{(\partial_x\varphi)^2}{2} + V\left(\frac{x}{\varepsilon}\right) + V_e(x) = 0, \qquad \partial_t(A^2) + \partial_x(A^2\ \partial_x\varphi) = 0. \tag{8}$$

The phase φ evolves according to a nonlinear Hamilton-Jacobi equation whose Hamiltonian $\mathcal{H}(x, x/\varepsilon, p) = p^2/2 + V(x/\varepsilon) + V_e(x)$ contains a fine-scale term. The intensity of the plane wave $|\psi|^2 = A^2$ evolves in time according to a linear conservation law whose velocity field is given by the x-derivative of φ. Still, this system needs to be homogenized in order to describe the limit behaviour as $\varepsilon \to 0$ of (6); such a theory exists up to now only in the context of viscosity solutions, see [38, 20, 21], which does not fully describe the dispersive structure of (7).

2.1. WKB expansion and emergence of the Bloch spectrum

As we just saw, the naive ansatz doesn't have the correct structure as it leads to a system where the small parameter ε keeps on being present. Hence following [6, 30], a refinement can be proposed considering a two-scale amplitude:

$$A\Big(t, x, y = \frac{x}{\varepsilon}\Big) = A_0(t,x,y) + \varepsilon A_1(t,x,y) + \cdots; \qquad A\Big(t, x, y + \frac{2\pi}{\varepsilon}\Big) = A(t,x,y). \tag{9}$$

Taking this new dependence into account inside (6) yields the expression:

$$\begin{aligned} -A\partial_t\varphi + \frac{1}{2}\Big(\partial_{yy}A - A(\partial_x\varphi)^2 + 2i(\partial_x\varphi)(\partial_y A)\Big) - \Big(V(y) + V_e(x)\Big)A \\ + \frac{i\varepsilon}{2}\Big(2\partial_t A + A\partial_{xx}\varphi + 2\partial_x A\ \partial_x\varphi - 2i\partial_{xy}A\Big) + \frac{\varepsilon^2}{2}\partial_{xx}A = 0. \end{aligned} \tag{10}$$

- The first step is to compare the $O(1)$ terms; this concerns A_0

$$\frac{1}{2}\partial_{yy}A_0 - V(y)A_0 + \left(i(\partial_x\varphi)(\partial_y A_0) - \frac{1}{2}A_0(\partial_x\varphi)^2\right) = A_0\big(\partial_t\varphi + V_e(x)\big).$$

As we shall see below, this means that $\partial_t\varphi+V_e$ has to be an eigenvalue associated to the eigenfunction A_0 for a certain time-independent Schrödinger operator. Indeed, let us consider the quantum mechanical momentum operator $\hat{p} = i\partial_y$ and look at the eigenmodes of $\mathcal{H}(y,\hat{p}) = -\frac{1}{2}\partial_{yy} + V(y)$ written in the Bloch-wave form $\Psi_\kappa(y) = \exp(i\kappa y)z_\kappa(y)$ for some real wave-number κ and a 2π-periodic modulation z_κ. Then if Ψ_κ satisfies

$$\forall y \in \mathbb{R}, \qquad \mathcal{H}(y,\hat{p})\Psi_\kappa = -\frac{1}{2}\partial_{yy}\Psi_\kappa + V(y)\Psi_\kappa = E(\kappa)\Psi_\kappa, \tag{11}$$

it easily follows that the envelope z_κ solves:

$$-\frac{1}{2}\partial_{yy}z_\kappa + V(y)z_\kappa - \left(i\kappa\partial_y z_\kappa - \frac{\kappa^2}{2}z_\kappa\right) = E(\kappa)z_\kappa.$$

Thus $O(1)$ terms inside (10) cancel if and only if $y \mapsto A_0(t,x,y)\exp(i\kappa y)$ is an eigenstate of $\mathcal{H}(y,\hat{p})$ associated to the eigenvalue $E(\partial_x\varphi) = -\partial_t\varphi - V_e(x)$:

$$\mathcal{H}(y,\hat{p})(A_0\exp(i\kappa y)) = -\big(\partial_t\varphi + V_e(x)\big)\ (A_0\exp(i\kappa y)), \qquad \kappa = \partial_x\varphi.$$

Note that the slow variable x shows up only as a parameter. Written in a more compact form, an Hamilton-Jacobi equation has been derived, where the fine scale $y = x/\varepsilon$ has disappeared:

$$\partial_t\varphi + E(\partial_x\varphi) + V_e(x) = 0. \tag{12}$$

- The second step consists in writing $A_0(t,x,y) = a_0(t,x)z_\kappa(y)$ with stationary orthonormal modulations: $\|z_\kappa\|_{L^2(0,2\pi)} = 1$. Hence comparing $O(\varepsilon)$ terms inside (10) taking into account (9) has been shown in [30] to be equivalent to the linear conservation law:

$$\partial_t(a_0)^2 + \partial_x\Big((a_0)^2\ E'(\partial_x\varphi)\Big) = 0. \tag{13}$$

All in all, starting from the Schrödinger equation (6), one has to consider the Bloch spectral decomposition (11) producing a countable set of distorted plane waves Ψ_κ^n, $n \in \mathbb{N}$, associated to the energy bands $E_n(\kappa)$. Then a convenient n^{th} band ansatz reads

$$\tilde{\psi}_n^\varepsilon(t,x) = a_n(t,x)\exp\left(\frac{i\varphi(t,x)}{\varepsilon}\right)\ z_\kappa^n(x/\varepsilon), \qquad \kappa = \partial_x\varphi(t,x), \tag{14}$$

where the unknowns evolve according to the n^{th} band WKB system (12)–(13)

$$\partial_t\varphi + E_n(\partial_x\varphi) + V_e(x) = 0; \qquad \partial_t\mu + \partial_x\Big(E_n'(\partial_x\varphi)\ \mu\Big) = 0, \quad \mu = (a_n)^2. \tag{15}$$

So $|\tilde{\psi}_n^\varepsilon|^2 = \mu|z_{\partial_x\varphi}^n|^2$ and the WKB expansion is used for the transient computation of a plane wave, the modulation z_κ evolving only through the relation $\kappa = \partial_x\varphi$. In the next subsection, we shall focus on the Bloch wave decomposition from both theoretical and computational points of view. Note that system (15) can recover the exact solution of (1) in case the dispersive term in (7) is zero. This happens for n^{th} band wavepackets which read like

$$\psi^\varepsilon(x) = \int_B \exp(i\kappa x/\varepsilon) z_\kappa^n(x/\varepsilon).d\kappa,$$

for which $a_0 \equiv 1$. In the special case $V_e \equiv 0$ and $\psi^\varepsilon(t=0,x) = \exp(i\kappa x/\varepsilon) z_\kappa^n(x/\varepsilon)$, both (15) and (1) furnish $\psi^\varepsilon(t,x) = \int_B \exp(i(\kappa x - E_n(\kappa)t)/\varepsilon) z_\kappa^n(x/\varepsilon).d\kappa$.

2.2. Derivation of the Sturm-Liouville eigenmodes

We begin by recalling the:

THEOREM 2.1. (**Bloch's Theorem**, *[7]*)
Let the potential V be 2π-periodic. Then each eigenstate Ψ of $\mathcal{H}(y,\hat{p}) = -\frac{1}{2}\partial_{yy} + V(y)$ satisfies $\Psi(y+2\pi) = \exp(2i\kappa\pi)\Psi(y)$ for all $y \in \mathbb{R}$ and some value $\kappa \in [-\frac{1}{2}, \frac{1}{2}]$.

Its proof is based on the fact that $\mathcal{H}$ commutes with the y-translation operator $\tau_{\pm 2\pi}$; then any eigenstate of $\mathcal{H}$ is also one of $\tau_{\pm 2\pi}$ for some complex eigenvalue. An important role is played by functions having phase-shifts when translated of 2π.

DEFINITION 2.1. (**κ-quasiperiodic functions**)
Any function $\Psi \in C^0(\mathbb{R})$ satisfying $\Psi(y+2\pi) = \exp(2i\kappa\pi)\Psi(y)$ for all $y \in \mathbb{R}$ is called a κ-quasiperiodic function.

Obviously a 0-quasiperiodic function is 2π-periodic. There are decomposition and synthesis relations for functions of this kind in $L^2(\mathbb{R})$, see [23, 43] for instance. We now define $\mathcal{H}_\kappa$ as the steady operator $\mathcal{H}$ restricted to κ-quasiperiodic functions for some $\kappa \in B$. Its spectral structure is well-known, see *e.g.* [43]; one has to find all the pairs $\{E_n(\kappa), \Psi_\kappa^n;\ \kappa \in]-\frac{1}{2}, \frac{1}{2}[\}$ for $n \in \mathbb{N}$ satisfying

$$\forall y \in \mathbb{R}, \qquad \begin{cases} -\dfrac{1}{2}\partial_{yy}\Psi_\kappa^n + V(y)\Psi_\kappa^n = E_n(\kappa)\Psi_\kappa^n, \\ \Psi_\kappa^n \text{ and } \partial_y \Psi_\kappa^n \text{ are } \kappa-\text{quasiperiodic.} \end{cases} \tag{16}$$

For any fixed $\kappa \in B$, there exists a complete set of eigenfunctions Ψ_κ^n orthonormal in $L^2(0,2\pi)$ with countably many eigenvalues $E_1(\kappa) < E_2(\kappa) < \cdots < E_{n-1}(\kappa) < E_n(\kappa) < \cdots$. The set $\{E_n(\kappa);\ \kappa \in]-\frac{1}{2}, \frac{1}{2}[\}$ is called the n^{th} energy band of $\mathcal{H}$ whereas Ψ_κ^n is a n^{th} Bloch function (or Bloch state). We also have for all κ, $E_n(\kappa) \to +\infty$ as $n \to +\infty$ and each map $\kappa \mapsto E_n(\kappa)$ is 1-periodic. The Bloch states Ψ_κ^n have the form already encountered in §2.1: $\Psi_\kappa^n(x) = \exp(i\kappa x) z_\kappa^n(x)$ for a certain 2π-periodic modulation. Now we notice that a scaling argument gives straightforwardly:

$$\mathcal{H}(y,\hat{p})\Psi_\kappa^n(y) = E_n(\kappa)\Psi_\kappa^n(y) \Leftrightarrow \mathcal{H}(x/\varepsilon, \varepsilon\hat{p})\Psi_\kappa^n(x/\varepsilon) = E_n(\kappa)\Psi_\kappa^n(x/\varepsilon),$$

Moreover, $\Psi_\kappa^n(./\varepsilon)/\sqrt{\varepsilon}$ is still orthonormal in $L^2(0, 2\varepsilon\pi)$.

In order to carry out the WKB program outlined in §2.1, an important stepping stone is the Bloch decomposition of $\mathcal{H}$ for all $\kappa \in B$. There exists several methods to do so: among them, one consists in solving directly the Sturm-Liouville problem (16), see [50], while another one relies on semiclassical quantization rules following [35, 17] (see also [15]). We turn to a spectral approach, taking advantage of the free package SciLab (available at `http://www-rocq.inria.fr/scilab`) as in [36]. We consider for now the potential $V \in C^1_{per}(\mathbb{R})$ and expand it in its Fourier series:

$$V(y) = \sum_{j\in\mathbb{Z}} V_j \exp(ijy), \qquad V_j = \frac{1}{2\pi}\int_0^{2\pi} V(y)\exp(-ijy).dy. \tag{17}$$

Since $\Psi^n_\kappa(y) = \exp(i\kappa y) z^n_\kappa(y)$ with $z^n_\kappa(y+2\pi) = z^n_\kappa(y)$, any Bloch state can also be expanded in plane waves written in Dirac's notation:

$$\forall (n,\kappa) \in \mathbb{Z} \times \left[-\frac{1}{2}, \frac{1}{2}\right], \qquad |n, \kappa >= \exp(i(n+\kappa)y).$$

Hence we have in mind to approximate the differential Sturm-Liouville equation (16) by an eigenvalue problem for the matrix H_κ defined as follows with $N \in \mathbb{N}$:

$$H_\kappa = \Big(< n', \kappa | \mathcal{H}_\kappa | n, \kappa > \Big)_{n,n'}; \qquad \kappa \in \left[-\frac{1}{2}, \frac{1}{2}\right], \quad n, n' \in \{-N, \cdots, N\}.$$

The kinetic energy entries are easily calculated:

$$-\frac{1}{2\pi}\int_0^{2\pi} \exp(-i(n+\kappa)y)\frac{1}{2}\partial_{yy}\exp(i(n'+\kappa)y).dy = \frac{1}{2}(n+\kappa)(n'+\kappa)\delta_{n,n'},$$

with $\delta_{n,n'}$ the classical Christoffel symbol. The potential is to be treated the same way and using its Fourier coefficients, one finds easily a Toeplitz representation

$$< n', \kappa | V(y) | n, \kappa >= \frac{1}{2\pi}\int_0^{2\pi} V(y)\exp(-i(n-n')y).dy = V_{n-n'},$$

which in turn leads to an eigenvalue problem for the following matrix:

$$H_\kappa = \begin{pmatrix} V_0 + \frac{1}{2}(\kappa - N)^2 & \bar{V}_1 & \cdots & \bar{V}_N \\ V_1 & V_0 + \frac{1}{2}(\kappa - N + 1)^2 & & \vdots \\ \vdots & & \ddots & \bar{V}_1 \\ V_N & \cdots & V_1 & V_0 + \frac{1}{2}(\kappa + N)^2 \end{pmatrix}. \tag{18}$$

We notice that since $V(x) \in \mathbb{R}$, $V_{-j} = \bar{V}_j$ and H_κ is Hermitian. If V is even, it is real symmetric and optimized algorithms can be used.

A simple and important case is the so-called Mathieu's equation corresponding to (16) with $V(x) = \cos(x)$; all the V_j's are zero except $V_{\pm 1} = \frac{1}{2}$. The outcoming matrix H_κ is tridiagonal symmetric for all $\kappa \in B$. This technique applies also to the so-called Kronig-Penney's model, [37], with discontinuous potential,

$$V(y) = 1 - \sum_{j\in\mathbb{Z}} \mathbf{1}_{y \in [\frac{\pi}{2} + 2j\pi, \frac{3\pi}{2} + 2j\pi]}, \tag{19}$$

and $\mathbf{1}_A$ stands for the characteristic function of a set A. The lattice atoms are meant to be in $\pi(1 + 2\mathbb{Z})$. Its corresponding Fourier coefficients are:

$$V_0 = \frac{1}{2}, \qquad V_j = \frac{\sin(j\pi/2)}{j\pi}.$$

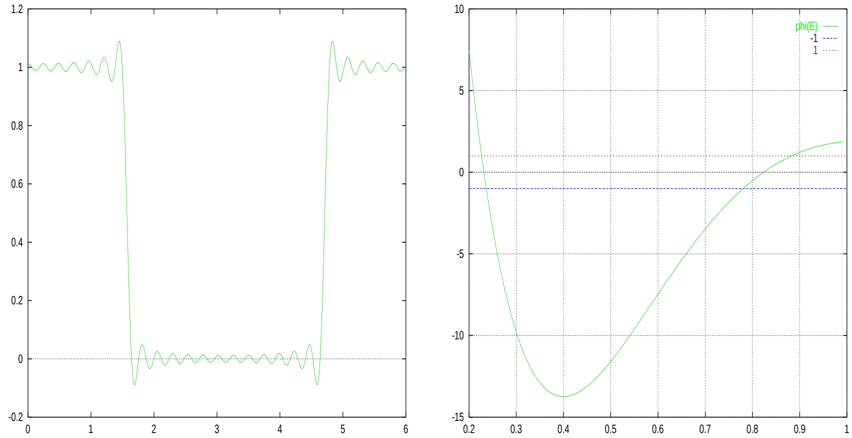

FIG. 1. Gibbs phenomenon for the potential (19) (left) and graph of $\phi(E)$ (20) (right).

In this case, the H_κ matrix is still real symmetric but full since all frequencies are present (however, harmonics decay like $O(1/|j|)$). The main feature of this model lies in the fact it can be solved exactly; the first bands $E_n(\kappa) \in [0,1]$ corresponding to bound eigenstates are solutions of the equation

$$\phi(E) = \frac{1-2E}{2\sqrt{E(1-E)}} \sinh(\beta\pi)\sin(\alpha\pi) + \cosh(\beta\pi)\cos(\alpha\pi) = \cos(2\pi\kappa), \quad (20)$$

with $\alpha = \sqrt{2E}$ and $\beta = \sqrt{2(1-E)}$. The next ones $E_n(\kappa) > 1$ which correspond to the classical regime satisfy:

$$\tilde{\phi}(E) = \frac{1-2E}{2\sqrt{E(1-E)}} \sin(\beta\pi)\sin(\alpha\pi) + \cos(\beta\pi)\cos(\alpha\pi) = \cos(2\pi\kappa). \quad (21)$$

For both examples, we display the numerical results $\kappa \mapsto E_n(\kappa)$ for $n = 1, \cdots, 5$ on Fig.2 where we chose the size of the matrix H_κ to be 61×61. Then we show in Fig.1 the resulting Fourier approximation of (19) together with the graph of $\phi(E)$. One can observe that the numerically computed first two energy bands are correctly located. The band gaps are known to be of the order of V_j, [3]. Of course, the discrete eigenvectors of the matrix H_κ are the Fourier coefficients of the modulations z_κ^n; we display in Fig.3 the square of these modulations for the five first bands and $\kappa = 0$. One can therefore observe the noticeable difference between the two bound states associated to the valence bands which are tightly sticked to the atoms. In sharp contrast, the first conduction band shows very small position density in the vincinity of the atoms. As $E_n(\kappa)$ increases, one arrives in the classical regime and position densities of the corresponding Bloch states are less peaked.

2.3. Band transport equations

Typically, the Hamilton-Jacobi equation (12) (with $E = E_n$ for some value n of the band index) develops caustics in finite time, *i.e.* sets of singularities for the phase φ. Therefore the WKB expansion is supposedly limited to local-in-time approximations of the wave function and its quadratic observables when classical

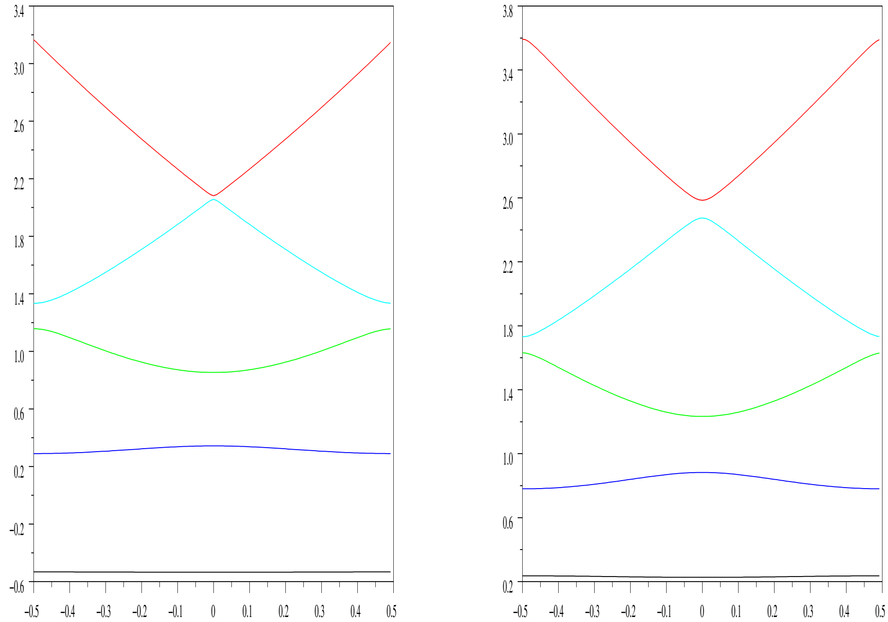

FIG. 2. Band structures for Mathieu's equation (left) and Kronig-Penney's model (right).

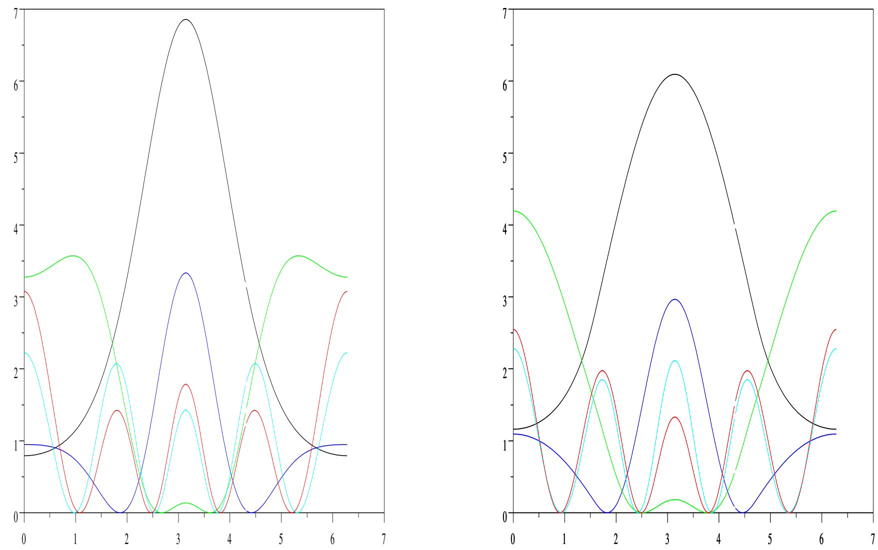

FIG. 3. Modulations $\left(z^n_{\kappa=0}(x)\right)^2$ associated to the bands of Fig.2.

singlevalued solutions of (12) are considered. Going beyond caustic onset is facilitated by "unfolding the caustics in phase space", [32]: this can be carried through relying on (band) Wigner transforms and their weak limits, the so-called (band) Wigner measures, as done in [23, 39, 43, 46]. We now present a short summary of these results, focusing on what will be needed from a computational standpoint.

Let us first notice that the Bloch spectral problem (16) induces an orthogonal decomposition of the state space into wavepacket subspaces:

$$L^2(\mathbb{R}) = \oplus_{n=1}^{\infty} \mathcal{S}_n^\varepsilon, \qquad \mathcal{S}_n^\varepsilon = \left\{ \phi_n^\varepsilon(x) = \int_B \sigma(\kappa)\Psi_\kappa^n(x/\varepsilon).\frac{d\kappa}{\sqrt{\varepsilon}};\ \sigma \in L^2(B) \right\}.$$

Indeed one can write any function $\psi \in L^2(\mathbb{R})$ as

$$\psi(x) = \sum_{n=1}^{\infty} \psi_n^\varepsilon(x), \qquad \psi_n^\varepsilon \in \mathcal{S}_n^\varepsilon, \tag{22}$$

together with:

$$\psi_n^\varepsilon(x) = \int_{-1/2}^{1/2} \hat{\psi}^\varepsilon(\kappa,n)\Psi_\kappa^n(x/\varepsilon).\frac{d\kappa}{\sqrt{\varepsilon}}, \quad \hat{\psi}^\varepsilon(\kappa,n) = \int_{\mathbb{R}} \psi(x)\bar{\Psi}_\kappa^n(x/\varepsilon).\frac{dx}{\sqrt{\varepsilon}}. \tag{23}$$

The Schödinger equation (6) with $V_e \equiv 0$ decouples into a series of "band equations":

$$i\varepsilon\partial_t\psi_n^\varepsilon = E_n(\varepsilon D)\psi_n^\varepsilon, \qquad n = 1, 2, ..., \tag{24}$$

where $E_n(\varepsilon D)$ is the pseudo-differential operator with Fourier multiplier $E_n(\varepsilon\kappa)$. The crucial feature that $E_n(\varepsilon D)$ leaves invariant the bandspace $\mathcal{S}_n^\varepsilon$ is generally lost when an exterior potential V_e is incorporated. The initial datum for (24) is obtained by L^2 projection of the initial wave function on each band space $\mathcal{S}_n^\varepsilon$ following (22)–(23). Then one sets up the band Wigner series $w_n^\varepsilon(t,x,\kappa)$ as in (3) for each ψ_n^ε and computes the corresponding time evolution equations from (24). It is meaningful to pass to the semiclassical limit $\varepsilon \to 0$ under the assumption that the nonnegative Borel measures

$$\forall n \in \mathbb{N}, \qquad w_{n,I}(x,\kappa) = \lim_{\varepsilon\to 0} w_n^\varepsilon(t=0,x,\kappa),$$

(where limits are possibly taken along subsequences) vanish on $\mathbb{R} \times C$, C standing for the set of band-crossing points. We thus obtain the transport equations for the limiting nonnegative bounded measures $w_n := \lim_{\varepsilon\to 0} w_n^\varepsilon$ as announced in (4), see [43, 23] for more details:

$$\forall n \in \mathbb{N}, \qquad \partial_t w_n(t,x,\kappa) + E_n'(\kappa)\partial_x w_n(t,x,\kappa) = 0. \tag{25}$$

This Cauchy problem is solved easily for $t > 0$, $\kappa \in B$ and $x \in \mathbb{R}$,

$$w_n(t,x,\kappa) = w_{n,I}\Big(x - t.E_n'(\kappa), \kappa\Big),$$

and (for instance) the position density $\rho^\varepsilon(t,x)$ homogenizes in the following way:

$$\rho^\varepsilon(t,x) \overset{\varepsilon \to 0}{\rightharpoonup} \rho(t,x) = \int_B \sum_{n=1}^{\infty} w_{n,I}(x - t.E_n'(\kappa), \kappa).d\kappa.$$

Assume now that the initial wave function is of the WKB type,

$$\psi(t=0,x) = \sqrt{\rho_I(x)}\exp(i\varphi_I(x)/\varepsilon),$$

where $\rho_I \in \mathbb{R}^+$ and $\varphi_I \in \mathbb{R}$ are smooth functions. It is an easy exercise to show that the weak limit of the band-Wigner function (3) associated to $\psi(t=0,.)$ as $\varepsilon \to 0$ is the monokinetic phase space measure,

$$w_n(t=0,x,\kappa) = \rho_I(x)\delta_\#\Big(\kappa - \partial_x\varphi_I(x)\Big), \tag{26}$$

where $\delta_\#$ stands for the 2π-periodic Dirac distribution: $\delta_\# = \sum_{j\in\mathbb{Z}} \delta(. - 2j\pi)$.

Denote by $\mathcal{I}_n^\varepsilon$ the orthogonal $L^2(\mathbb{R})$-projector onto each one of the band-spaces $\mathcal{S}_n^\varepsilon$ defined at the beginning of this section and by $w_{n,I}^\varepsilon$ the band Wigner transform of $\mathcal{I}_n^\varepsilon\psi(t=0,.)$. If all the bands E_n are isolated (which is possible in one space dimension), there holds [23], §4:

$$w(t=0,x,\kappa) = \sum_{n\in\mathbb{N}} w_{n,I}(t=0,x,\kappa), \qquad w_{n,I}^\varepsilon \overset{\varepsilon \to 0}{\rightharpoonup} w_{n,I}.$$

Since each $w_{n,I}$ is a bounded nonnegative measure, we conclude that it is supported inside the Lagrangian manifold $\{(x,\varphi_I(x)+2j\pi);\ x \in \mathbb{R}, j \in \mathbb{Z}\}$. Hence we have "band monokinetic initial data":

$$\forall n \in \mathbb{N}, \qquad w_n^0(t=0,x,\kappa) = \rho_{n,I}(x)\delta_\#\Big(\kappa - \partial_x\varphi_I(x)\Big). \tag{27}$$

In order to highlight consistency with the WKB ansatz (14), let us consider the WKB initial wave function

$$\tilde\psi_{n,I}^\varepsilon(x) = a_{n,I}(x)\exp(i\varphi_I(x)/\varepsilon)z^n_{\partial_x\varphi_I}(x/\varepsilon). \tag{28}$$

At first sight, $\tilde\psi_{n,I}^\varepsilon \notin \mathcal{S}_n^\varepsilon$ for general φ_I and $a_{n,I}$; but since

$$\forall n \in \mathbb{N}, \qquad |z_\kappa^n(x/\varepsilon)|^2 \overset{\varepsilon \to 0}{\rightharpoonup} Z^n \in \mathbb{R}^+,$$

uniformly for $\kappa \in B$, a simple computation shows that the Wigner series $\tilde w_{n,I}^\varepsilon$ associated to (28) satisfies:

$$\tilde w_{n,I}^\varepsilon(x,\kappa) \overset{\varepsilon \to 0}{\rightharpoonup} |a_{n,I}(x)|^2 Z^n \delta_\#\Big(\kappa - \partial_x\varphi_I(x)\Big).$$

And what we obtain is nothing but monokinetic band Wigner measures of the type (27). Very recently, nonvanishing external potentials have been included in the analysis [31]; in this last case, the transport equation (25) is of Vlasov type and reads

$$\forall n \in \mathbb{N}, \qquad \partial_t w_n + E_n'(\kappa)\partial_x w_n - V_e'(x)\partial_\kappa w_n = 0. \tag{29}$$

One recovers the Hamilton-Jacobi equation (12) from (25) by assuming furthermore that the n^{th} band Wigner measure is monokinetic (27) [13, 23]. Hence each of the n^{th} band position densities satisfies a scalar conservation law whose velocity field is precisely $E_n(\partial_x\varphi)$ if restricted to the time interval before caustic onset, [46, 13, 1]. Also the limiting n^{th} band density ρ_n is precisely the limit (as $\varepsilon \to 0$) of the sequence ρ_n^ε associated to (14)-(15):

$$\forall n \in \mathbb{N}, \qquad \rho_n^\varepsilon := |\tilde{\psi}_n^\varepsilon|^2 \overset{\varepsilon \to 0}{\rightharpoonup} |a_n|^2 Z_n := \rho_n,$$

at least before caustic onset. We remark that the characteristics curves of the kinetic equation (25)–(26) are the Hamiltonian trajectories in phase space, ($\dot{}$ standing for time-differentiation)

$$\dot{X} = E_n'(K), \qquad \dot{K} = -V_e'(X), \tag{30}$$

along which the Borel measure w_n remains constant. Taking as an initial data

$$K(0) = \partial_x \varphi_I(X(0)), \qquad X(0) = X \in \mathbb{R},$$

ones recovers precisely the rays of the Hamilton-Jacobi equation (12). Thus, from the standpoint of the semiclassical problem (6), this nonlinear equation becomes meaningless if globally understood in a monovalued (*i.e.* classical or viscosity) sense. Instead, a concept of multivalued solution relying on the validity of the bicharacteristics $t \mapsto (X,K)(t)$ associated to both the equation (12) and the Hamiltonian system (30) beyond caustic onset must be considered. Hence the monokinetic density is replaced by a linear superpostion:

$$w(t,x,\kappa) = \sum_{k=1}^{N} \rho_k(t,x)\delta_{\#}\Big(\kappa - \partial_x\varphi_k(t,x)\Big), \qquad \partial_x\varphi_k = u_k. \tag{31}$$

However, solutions of this kind are delicate to handle computationally, [45, 33, 29, 10], because it amounts to solving (or approximating by means of κ-moments) a transport equation in the sense of measures, see however [34]. Keeping in mind that our primary interest lies in the bicharacteristics of (30), (12) (or analogously the associated conservation law obtained by x-differentiation), we are about to show that they can be extracted from a simpler approach, namely the K-multivalued solutions in the sense of [12].

2.4. Introducing K-branch entropy solutions

In this subsection, we summarize the construction of nonnegative "multibranch solutions" of the Cauchy problem for 1D scalar balance laws with $uF'(u) \geq 0$

$$\partial_t u + \partial_x F(u) + G'(x) = 0, \tag{32}$$

under the nondegeneracy condition

$$\Big|\Big\{\xi \in \mathbb{R} \text{ such that } \tau + F'(\xi)\zeta = 0\Big\}\Big| = 0, \qquad (\tau,\zeta) \neq 0,$$

through a kinetic formulation as in [12], see also [40, 41, 48, 49]. Let $K \in \mathbb{N}$,

$$\Theta_K := \Big\{ \theta \in C^0(\mathbb{R}); \qquad \partial_\xi^K \theta(\xi) \geq 0 \qquad \text{in } \mathcal{D}'(\mathbb{R}) \Big\},$$

are test-functions and, for some $L \in \mathbb{R}^+$,

$$\mathcal{F}_L := \Big\{ f \in L^\infty, \quad 0 \leq f \leq 1 \text{ a.e. with } Supp_\xi(f) \subset [0, L] \Big\}$$

is a set of bounded kinetic densities with finite speed of propagation. Each $f \in \mathcal{F}_L$ induces a moment vector $\vec{m}(f) \in \mathbb{R}^K$ with components:

$$m_k(f) = \int_{\mathbb{R}+} \xi^{k-1} f(\xi).d\xi, \qquad k = 1, \ldots, K. \tag{33}$$

It is therefore possible to define the set of "realizable moments",

$$\mathbf{M}_K^L = \Big\{ \vec{m} \in \mathbb{R}^K ; \exists f \in \mathcal{F}_L \text{ such that } \vec{m} = \vec{m}(f) \Big\},$$

on which one formulates the following minimization problem:

$$\mathbf{J}_K^\theta(\vec{m}) = \inf_{f \in \mathcal{F}_L} \left\{ \int_{\mathbb{R}+} \theta(\xi) f(\xi).d\xi \text{ where } \vec{m}(f) = \vec{m} \in \mathbf{M}_K^L \text{ and } \theta \in \Theta_K \right\}.$$

It is shown in [12] that for any $\vec{m} \in \mathbf{M}_K^L$, there exists a unique solution of this problem called the *K-branch Maxwellian*. The minimizer is independent of the test-function $\theta \in \Theta_K$. It is determined by a vector of nonnegative real numbers $\vec{u} = (u_1, ..., u_K)$ in decreasing order and reads

$$\mathcal{M}_{K,\vec{m}}(u_1, \ldots, u_K, \xi) = \sum_{k=1}^{K} (-1)^{k-1} H(u_k - \xi), \qquad u_k > u_{k+1} \geq 0, \tag{34}$$

where H stands for the Heaviside function. The "realizable moments" are given by the following map $\vec{m} : \ [0, L]^K \longrightarrow \mathbf{M}_K^L$

$$m_\ell(u_1, \ldots, u_K) := \frac{1}{\ell} \sum_{k=1}^{K} (-1)^{k-1} (u_k)^\ell, \qquad \ell = 1, \ldots, K. \tag{35}$$

It realizes a smooth one-to-one mapping of the u_k's as long as $u_k > u_{k+1}$ for all k under consideration. This leads to the following definition:

Definition 2.2. *(***K-multivalued solutions***, [12])*
Any measurable function $\{0, 1\} \ni f(t, x, \xi)$ *on* $\mathbb{R}^+ \times \mathbb{R} \times \mathbb{R}^+$ *satisfying the following kinetic equation in the sense of distributions*

$$\partial_t f + F'(\xi) \partial_x f - G'(x) \partial_\xi f = (-1)^{K-1} \partial_\xi^K \tilde{m}, \qquad f(t, x, \xi) = \mathcal{M}_{K, \vec{m}(f)}, \tag{36}$$

with $\tilde{m}$ *a nonnegative Radon measure on* $\mathbb{R}^+ \times \mathbb{R} \times \mathbb{R}^+$ *is a K-multivalued solution.*

Theoretical results for K-multivalued solutions are provided in [12, 48, 49]. For $K > 1$, K-multivalued solutions generalize Kružkov's notion of bounded entropy solution of (32); in the special cases $K = 1$ and $K = 2$, these statements coincide with the ones written in [40, 41]. There is also equivalence between the kinetic equation and the hyperbolic system acting on the "realizable moments".

THEOREM 2.2. *(Brenier & Corrias, [12])*
A measurable function $\mathcal{F}_L \ni f(t,x,\xi) = \sum_{k=1}^{K}(-1)^{k-1}H(u_k(t,x)-\xi)$ *is a K-multivalued solution if and only if the entropy inequalities hold in* $\mathcal{D}'(\mathbb{R}^+\times\mathbb{R})$ *for any* $\theta \in \Theta_K$*:*

$$\partial_t \int_{\mathbb{R}^+} \theta(\xi)f(\xi).d\xi + \partial_x \int_{\mathbb{R}^+} F'(\xi)\theta(\xi)f(\xi).d\xi + G'(x)\int_{\mathbb{R}^+}\theta'(\xi)f(\xi).d\xi \le 0. \quad (37)$$

Equality holds in case $\partial_\xi^K \theta \equiv 0$.

For $\theta(\xi) = \xi^\ell$, $\ell = 0, 1, \cdots, K-1$, one gets therefore a set of K equations. It has been shown in [29] that this system is equivalent to the moment system obtained from (25)-(31) as long as K is big enough to keep $\vec{m} \equiv 0$ in (36); more precisely, one has: (see also Theorem 3.5 in [12]).

THEOREM 2.3. *(***Equivalence of moment systems***, [29])*
Let $\rho_I \equiv 1$, $u_I := \partial_x\varphi_I$ *a given smooth function in (26) and for some* $n \in \mathbb{N}$, $\tilde{w}_n(t,x,\xi)$ *be the solution of the Liouville equation (29) with initial condition,* $\tilde{w}_n(0,x,\xi) = H(\xi - u_I(x))$. *Consider the set:*

$$\mathcal{C} = \Big\{\xi \in \mathbb{R}^+ \text{ such that } \tilde{w}_n(t,x,\xi) = 1,\ \tilde{w}_n(0,x,\xi) = H(\xi - u_I(x))\Big\}.$$

Assume that $\mathcal{C}$ *has only* M *connected components. If*
- $M = \frac{1}{2}(K+1)$ *(K odd) or* $M = K/2$ *(K even),*
- $N = K$ *in (31),*

then the moment system obtained from (29)-(31) and the H-system obtained from (29)-(34) with $\theta(\xi) = \xi^\ell$, $\ell = 0, 1, \cdots, K-1$ *produce the same velocities* $u_k(t,x)$.

The system (37) is genuinely nonlinear and diagonalizes in Riemann coordinates; for smooth solutions, the u_k's appearing in (34) are strong Riemann invariants and each one satisfies (32). System (37) is *strictly* hyperbolic if and only if they are all distinct; in this case, $u_k > u_{k+1}$ and the map $\vec{m}$ (35) is a diffeomorphism.

DEFINITION 2.3. *(***K-branch entropy solutions***)*
A K-branch entropy solution of (32) is any set $\vec{u}$ *of* K *nonnegative measurable functions* $u_k(t,x)$ *in* $L^\infty(\mathbb{R}^+\times\mathbb{R})$ *such that* $u_k > u_{k+1}$ *and for which (37) holds with* $f(t,x,\xi) = \sum_{k=1}^{K}(-1)^{k-1}H(u_k(t,x)-\xi)$.

K-branch entropy solutions enjoy a "finite superposition principle" as shown in [45] since they match the solutions by characteristics [1, 11, 32] for K big enough.

This last property is of special interest since the WKB system (15) has to be understood as a Correspondence Principle between quantum and classical mechanics. Since the Hamilton-Jacobi equation produces a smooth but possibly multivalued solution, we interpret it relying on the preceding framework; differentiating in the space variable, we pass from (12) to an equation of the type (32):

$$\partial_t u + \partial_x E_n(u) + V_e'(x) = 0; \qquad F'(\xi) = E_n'(\xi),\ G'(x) = V_e'(x).$$

K-branch entropy solutions produce an approximation of order ε to (6)–(10) for K big enough as they are concerned only with (12); to complete the ansatz, (13) has to be processed too. Indeed we shall see in the next section how to deduce very easily the corresponding intensities μ so as to keep the equivalence result of Theorem 2.3 with the N densities ρ_k in (31). Let us mention that theoretical stability results are available in the strictly hyperbolic case and for $V_e' \in L^1 \cap L^\infty(\mathbb{R})$ as a byproduct of [2, 8, 24, 25, 27].

2.5. Fourier and parabolic band approximations

A genuine drawback is that the energy bands $\kappa \mapsto E_n(\kappa)$ aren't known analytically; so the derivation of fluxes of the type $\int_{\mathbb{R}^+} E_n'(\xi)\theta(\xi)f(\xi).d\xi$ inside the system (37) is not easy on a computational level. One way out will be to take advantage of the smoothness and symmetry of $E_n(\kappa)$ writing it as a Fourier series,

$$E(\kappa) = \frac{E_0}{2} + \sum_{j\in\mathbb{N}^*} E_j \cos(2\pi j\kappa), \qquad E_j = 4\int_0^{\frac{1}{2}} E(\kappa)\cos(2\pi j\kappa).d\kappa. \tag{38}$$

We shall also use a more standard procedure as our main interest lies only in simulating the dynamics of the last valence and the first conduction bands (the second and third ones on Fig.2). Namely, the so-called parabolic band approximation consists in writing them as quadratic functions of the wave-number, [3, 44]:

$$E_c(\kappa) \simeq E_c(0) + \frac{\kappa^2}{2m^*}, \qquad |\kappa| \ll \frac{1}{2}. \tag{39}$$

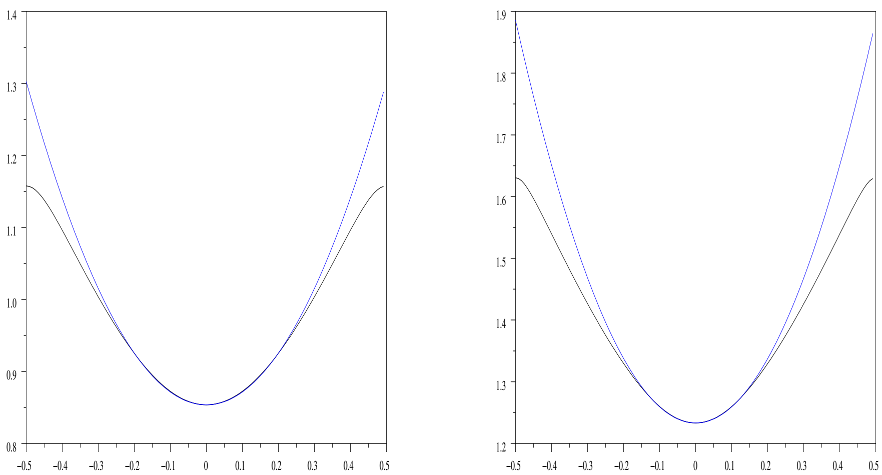

FIG. 4. Parabolic approximations associated to the third bands in Fig.2.

The number $m^* > 0$ is called the electron's effective mass and heavily depends on the potential V through the bands diagram. In the case $V(x) = \cos(x)$, one finds the numerical values which give a good approximation for $|\kappa| \le 0.3$,

$$m^* = 0.2783, \qquad E_c(0) = 0.8536,$$

whereas the Kronig-Penney's model seems to be more restrictive with $|\kappa| \le 0.2$ and

$$m^* = 0.1915, \qquad E_c(0) = 1.2332.$$

Therefore the WKB equations (15) boil down to

$$\partial_t \varphi + \frac{1}{2m^*}(\partial_x \varphi)^2 + V_e(x) = 0; \qquad \partial_t \mu + \frac{1}{m^*}\partial_x\Big(\mu\ \partial_x \varphi\Big) = 0, \quad \mu = (a_n)^2. \tag{40}$$

Of course, this system bears a lot of similarities with the one studied in [27]. So, interpreting (40) relying on [12] reads for $f(t,x,\xi) = \sum_{k=1}^{K} (-1)^{k-1} H(u_k(t,x) - \xi)$:

$$\partial_t \left(\int_{\mathbb{R}+} \xi^\ell f(\xi).d\xi \right)_{\ell=0,\dots,K-1} + \frac{1}{m^*}\ \partial_x \left(\int_{\mathbb{R}+} \xi^{\ell+1} f(\xi).d\xi \right)_{\ell=0,\dots,K-1} = \vec{0}. \tag{41}$$

We shall limit ourselves mainly to the cases $K = 2, 3$. The intensities have to be sought as *e.g.* duality solutions, [8], of the K continuity equations:

$$\partial_t(\mu_\ell) + \frac{1}{m^*}\ \partial_x(u_\ell\ \mu_\ell) = 0, \qquad \ell = 1, ..., K. \tag{42}$$

The initial data for (41) are modified by a small parameter $|\eta| \ll 1$ in order to keep the system in a strictly hyperbolic region, [27], and read:

$$u_\ell(t=0,x) = \partial_x \varphi(t=0,x) - \eta \left(\ell - \frac{K+1}{2} \right), \qquad \mu_\ell(t=0,x) = \mu(t=0,x).$$

3. NUMERICAL PROCESSING OF PARABOLIC BANDS

3.1. Computation of the velocities and their corresponding intensities

From now on, we assume that the external potential V_e vanishes identically and we consider a uniform cartesian grid determined by the two positive parameters Δx, Δt which stand for the mesh-size and the time-step respectively. We shall denote $x_j = j\Delta x$, $x_{j+1/2} = (j+1/2)\Delta x$, $t^n = n\Delta t$, and generic computational cells read

$$T_j^n = \left[t^n, t^{n+1}\right[\times \left[x_{j-\frac{1}{2}}, x_{j+\frac{1}{2}}\right[, \qquad (j,n) \in \mathbb{Z} \times \mathbb{N}.$$

As usual, the parameter λ will refer to $\Delta t / \Delta x$. Then, for a given $K > 1$, the grid functions $(\vec{m}_j^n, \vec{\mu}_j^n) \in (\mathbb{R}^K)^2$ stand for some numerical approximations of the moments in (41) $\vec{m}(t^n, x_j)$ and the intensities $\vec{\mu}(t^n, x_j)$ in (42) on each T_j^n. K-branch solutions are updated in time with an explicit Euler marching method:

$$\vec{m}_j^{n+1} = \vec{m}_j^n - \frac{\lambda}{2m^*}\Big(F_K(\vec{m}_j^n, \vec{m}_{j+1}^n) - F_K(\vec{m}_{j-1}^n, \vec{m}_j^n) \Big), \qquad j \in \mathbb{Z}.$$

Relying on previous experience, [27, 28, 29], we selected the simple *local Lax-Friedrichs* (LLxF for short) numerical flux vector which in the present setting reads:

$$\begin{aligned} F_K(\vec{m}_j^n, \vec{m}_{j+1}^n) \;=\; & \left\{ \frac{1}{\ell} \sum_{k=1}^{K} (-1)^{k-1} \Big[(u_k^\ell)_j^n + (u_k^\ell)_{j+1}^n \Big] \right\}_{\ell=2,\dots,K+1} \\ & - \max_{k;\; j,j+1} |u_k|^n \Big(\vec{m}_{j+1}^n - \vec{m}_j^n \Big). \end{aligned} \tag{43}$$

A crucial step lies clearly in finding out the relations between the moments m_k's and the Riemann coordinates u_k's; they constitute a Vandermonde system and have been solved in [45]. We recall briefly here the cases $K = 2$ and $K = 3$ since they correspond to the generic 1D singularities. From (35), we have

$$m_1 = u_1 - u_2, \qquad m_2 = \frac{1}{2}\Big((u_1)^2 - (u_2)^2 \Big),$$

and this can obviously be inverted,

$$u_1 = \frac{m_2}{m_1} + \frac{m_1}{2}, \qquad u_2 = \frac{m_2}{m_1} - \frac{m_1}{2},$$

in order to find the last component of the fluxes:

$$m_3 = \frac{1}{3}\Big((u_1)^3 - (u_2)^3 \Big) = \frac{(m_2)^2}{m_1} + \frac{(m_1)^3}{12}.$$

For $K = 3$, things get worse and following [45],

$$u_2 = \frac{-(m_1)^3 - 6m_3 + 6m_1 m_2}{3\big((m_1)^2 - 2m_2\big)}; \qquad u_{1,3} = \frac{4\big((m_1)^3 - 3m_3\big) \pm \sqrt{\Delta}}{12\big((m_1)^2 - 2m_2\big)}$$

where:

$$\Delta = 16\big((m_1)^3 - 3m_3\big)^2 - 24\big((m_1)^2 - 2m_2\big)\big((m_1)^4 + 12(m_2)^2 - 12m_3 m_1\big).$$

One can write $m_4 = \frac{1}{4}\big((u_1)^4 - (u_2)^4 + (u_3)^4\big)$ in terms of m_1, m_2, m_3 to close the system. At this point, one is able to propagate in time the $\vec{m}_j^n$ and thus the corresponding $\vec{u}_j^n$. We now explain how the intensities $\vec{\mu}_j^n$ can be deduced in order to keep the equivalence Theorem 2.3 true even for nontrivial initial densities ρ_I. The continuity equation of (40) implies for $k = 1, ..., K$,

$$\begin{gathered} \mu_k(t,x) = \mu_k(t=0,x_0) \left| \frac{\partial x_0}{\partial x} \right|, \\ x = x_0 + t.u_k(t=0,x_0)/m^* = x_0 + t.u_k(t,x)/m^*, \end{gathered}$$

since the Hamilton-Jacobi equation is homogeneous and its characteristics are straight lines along which the u_k's are constant. Hence for any $x \in \mathbb{R}$ and $t > 0$, the starting point x_0 is explicitly known when having the values $u_k(t,x)$:

$$x_0 = x - \frac{t.u_k(t,x)}{m^*} \;\Rightarrow\; \frac{\partial x_0}{\partial x} = 1 - \frac{t.\partial_x u_k(t,x)}{m^*}, \qquad k = 1, ..., K.$$

Numerically, if $\vec{u}_j^n$ is known up to $n = t^n/\Delta t$ this last expression rewrites:

$$\forall j \in \mathbb{Z}, \quad (\mu_k)_j^n = \mu\left(t = 0, x_j - \frac{t^n (u_k)_j^n}{m^*}\right) \left|1 - \frac{t^n}{2m^* \Delta x}\Big((u_k)_{j+1}^n - (u_k)_{j-1}^n\Big)\right|.$$

The accuracy of the intensities $\vec{\mu}_j^n$ is considerably improved when compared to the results obtained with finite-differences in [27, 28] and cheaper compared to [33, 45]. Concerning the initial datum, we selected $\eta = \Delta x/100$.

3.2. The Mathieu equation: $V(x) = \cos(x)$

As an illustration of the preceding statements, we consider in this section a simulation of (40)-(41) with $K = 3$ for initial data modeling self-interfering pulses:

$$u_0(x) = 0.3\sin(x), \qquad \mu_0(x) = \frac{1}{2\sqrt{\pi}}\Big(\exp(-(x - \frac{\pi}{2})^2) + \exp(-(x - \frac{3\pi}{2})^2)\Big).$$

The parameter 0.3 forces the K-branch solutions to remain inside the portion of the Brillouin zone where the parabolic approximation (39) holds true. The characteristic size of the wave-packet is determined by $\varepsilon = 0.2$. We selected $\Delta x = 0.03$, $\Delta t = 0.025$ and iterated the scheme (43) up to $T = 3$ to obtain Fig. 5. These results suggest that the rendering of the trivalued solution is consistent with the ray-traced picture (30) away from phase transitions, *i.e.* points where the solution bifurcates from one to three values simultaneously. At these locations, undercompressive shocks moving at characteristic speed appear in $\vec{m}(t,.)$, [27, 29]. The scheme (43) keeps away from these nonstrict hyperbolicity points and this has consequences on the intensities $\vec{\mu}(t,.)$. In order to check consistency with the genuine Schrödinger equation, we simulated (2), (14) by means of a Fourier solver to compare the position densities; see Fig.6. The "3-branch position density" is meant to be:

$$\begin{cases} \mu_2(t,x)|z^n_{u_2(t,x)}(x/\varepsilon)|^2 & \text{if } |(u_1+u_3) - 2u_2|(t,x) \le \eta, \\ \sum_{k=1}^3 \mu_k(t,x)|z^n_{u_k(t,x)}(x/\varepsilon)|^2 & \text{otherwise.} \end{cases}$$

We give here some details about the numerical unsplit solver we set up for solving (2), (14) in the special case $V(x) = \cos(x)$. The ansatz (14) reads

$$\tilde{\psi}_n^\varepsilon(t = 0, x) = \sqrt{\mu_0(x)}\exp(i\varphi_0(x)/\varepsilon) z^n_{u_0(x)}(x/\varepsilon), \qquad \partial_x \varphi_0(x) = u_0(x),$$

where $n = 3$ corresponds to the first conduction band (see Figs. 2 and 3). We select values for ε such that $1/\varepsilon$ belongs to $\mathbb{N}$ and expand $\psi(t,.)$ in its Fourier series for $x \in [0, 2\pi]$:

$$\psi(t,x) = \sum_{j\in\mathbb{Z}} \psi_j(t)\exp(ijx), \qquad \psi_j(t) = \frac{1}{2\pi}\int_0^{2\pi} \psi(t,x)\exp(-ijx).dx.$$

For all $t > 0$, the Fourier coefficients $\psi_j(t)$ satisfy the following differential system because for the Mathieu's equation, we have $V(x) = \frac{\exp(ix)+\exp(-ix)}{2}$:

$$\forall j \in \mathbb{Z}, \qquad i\varepsilon\dot{\psi}_j(t) = \frac{1}{2}\left(\psi_{j-\frac{1}{\varepsilon}}(t) + j^2\varepsilon^2\psi_j(t) + \psi_{j+\frac{1}{\varepsilon}}(t)\right). \tag{44}$$

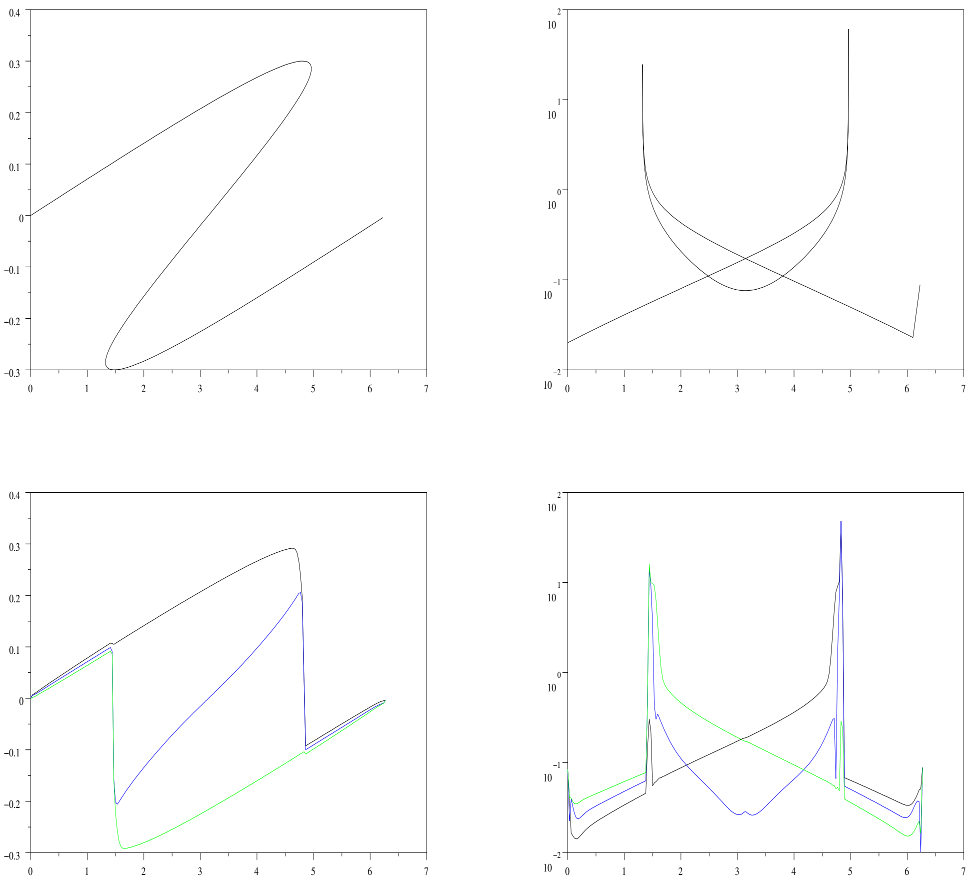

FIG. 5. Exact (top) vs. numerical (bottom) velocities $\vec{u}(t=3,.)$ and intensities $\vec{\mu}(t=3,.)$.

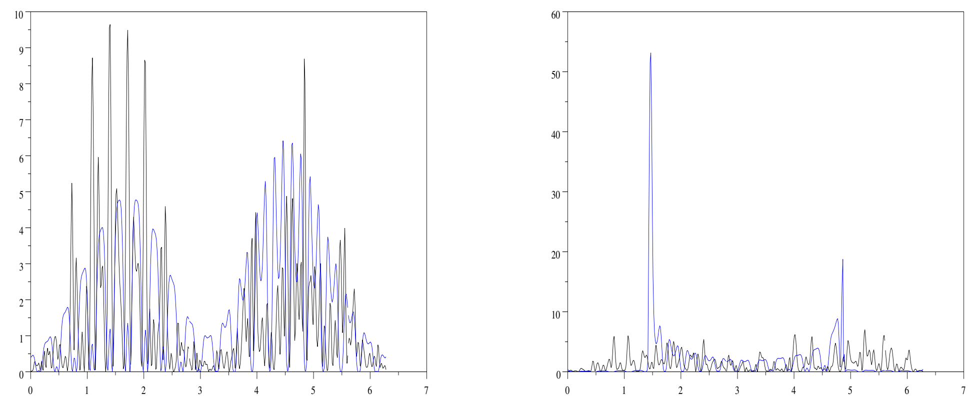

FIG. 6. Densities from Schrödinger and WKB, $\varepsilon = 0.05$; $T = 0.1$ (left) and $T = 3$ (right).

Of course, in practice, one has to consider a finite set of coefficients only, that is to say $\psi_j(t) \equiv 0$ for $|j| > M \in \mathbb{N}$. We chose $M = 75$ to produce the results of Fig. 6 together with $\Delta x = 0.013$ and $\Delta t = 0.01$. We present on Fig.7 the error on

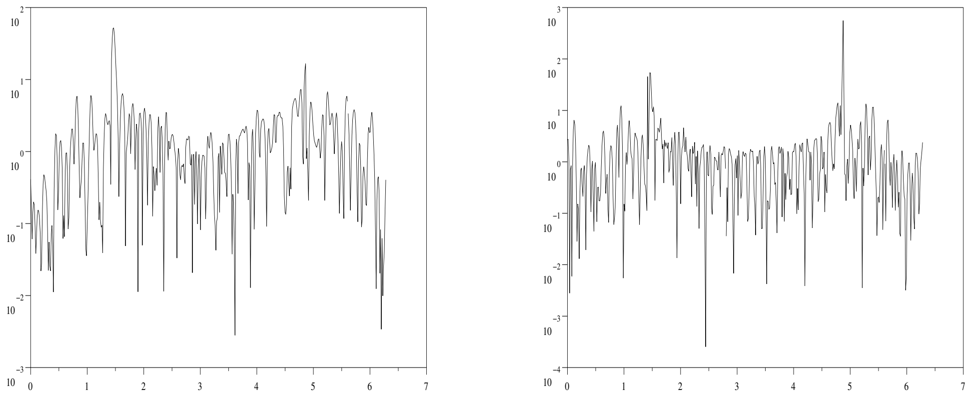

FIG. 7. Errors (45) on position densities in $T = 3$: $\varepsilon = 1/20$ (left), $\varepsilon = 1/50$ (right).

position densities

$$\ln \left| |\psi(T,x)|^2 - \sum_{k=1}^{3} \mu_k(T,x) |z^n_{u_k(T,x)}(x/\varepsilon)|^2 \right|, \tag{45}$$

for $T = 3$ and $\varepsilon = 1/20$, $\varepsilon = 1/50$, $\Delta x, \Delta t$ being held fixed.

4. COMPUTATIONS INSIDE THE WHOLE BRILLOUIN ZONE

4.1. Velocities and intensities derivation

It is clear looking at Fig. 4 that the parabolic band approximation is only valid for a portion of the Brillouin zone B whose size depends on the bands structure induced by $V(x)$. It can cover 60% of B for the Mathieu's equation, but is shrinks to less than 40% for the Kronig-Penney's model. Hence in order to carry out high field simulations, one can feel the need for a more sophisticate approach still based on K-branch entropy solutions but taking into account for the whole band structure. Indeed, as the first conduction band $\kappa \mapsto E(\kappa)$ is 1-periodic, even and smooth even at the edges of the Brillouin zone, it can be written as a Fourier series (38) where the coefficients E_j decay very quickly with $j \in \mathbb{N}$. We display on Fig. 8 the resulting approximation for the conduction bands in Fig. 2. In order to cope with the framework presented in §2.4, we have now to consider that $F'(u) = E'(u)$ in (32) and this leads us to slightly more intricate moment systems:

$$\partial_t \left(\int_{\mathbb{R}+} \xi^\ell f(\xi).d\xi \right)_{\ell=0,\dots,K-1} + \partial_x \left(\int_{\mathbb{R}+} \xi^\ell E'(\xi) f(\xi).d\xi \right)_{\ell=0,\dots,K-1} = \vec{0}. \tag{46}$$

Let us mention however that in this case, the resulting systems (46) are nonstrictly hyperbolic and nongenuinely nonlinear in the sense of Lax, [4]. We see that the

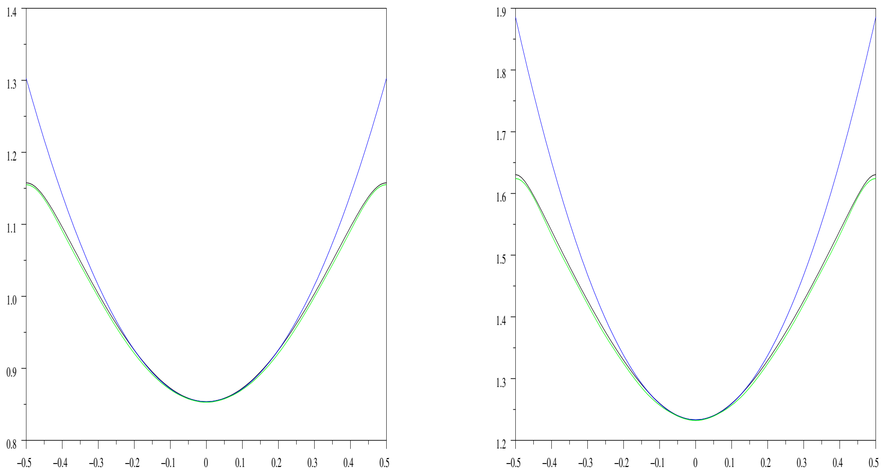

FIG. 8. Fourier and parabolic approximations associated to the third bands in Fig.2.

fluxes appearing in (46) are given by integrals of the form

$$\int_{\mathbb{R}^+} \xi^\ell E'(\xi) f(t,x,\xi).d\xi = \sum_{j\in\mathbb{N}^*} -E_j \int_{\mathbb{R}^+} 2\pi j \xi^\ell \sin(2\pi j\xi) f(t,x,\xi).d\xi,$$

where $\ell = 0, ..., K-1$ and $f(t,x,\xi) = \sum_{k=1}^K (-1)^{k-1} H(u_k(t,x)-\xi)$. It turns out that the right-hand side can be computed exactly with integrations by parts. For instance, in the cases $K = 2, 3$, one has for any $\lambda \in \mathbb{R}$,

$$\int_0^u \xi\lambda \sin(\lambda\xi).d\xi = -u\cos(\lambda u) + \frac{\sin(\lambda u)}{\lambda},$$
$$\int_0^u \xi^2\lambda \sin(\lambda\xi).d\xi = -u^2\cos(\lambda u) + \frac{2u\sin(\lambda u)}{\lambda} + \frac{2(\cos(\lambda u)-1)}{\lambda^2}.$$

We follow the same lines as in the preceding section; of course the numerical fluxes are more involved and one musts replace (43) with:

$$\begin{aligned} F_K(\vec{m}_j^n, \vec{m}_{j+1}^n) \;=\; & \left\{ \sum_{k=1}^K (-1)^{k-1} \Big(\int_0^{(u_k^\ell)_j^n} + \int_0^{(u_k^\ell)_{j+1}^n} \Big)\, \xi^{\ell-1} E'(\xi).d\xi \right\}_{\ell=1,\dots,K} \\ & - \max_{k;\; j,j+1} |E'(u_k)|^n \left(\vec{m}_{j+1}^n - \vec{m}_j^n \right). \end{aligned} \tag{47}$$

In order to complete the ansatz (14), we still have to deduce the values of $\vec{\mu}(t^n, x_j)$ for j, n in $\mathbb{Z}\times\mathbb{N}$. This will be done accordingly; for all k under consideration, we deduce from (13) that

$$\mu_k(t,x) = \mu_k(t=0, x_0) \left| \frac{\partial x_0}{\partial x} \right|, \qquad x = x_0 + t.E'(u_k(t,x)),$$

and this paves the way for recovering numerically the $\vec{\mu}_j^n$ out of the set of $\vec{u}_j^n$ for all $j \in \mathbb{Z}$, $k = 1, ..., K$, with the formula:

$$(\mu_k)_j^n = \mu\Big(t = 0, x_j - t^n E'\big((u_k)_j^n\big)\Big) \left| 1 - \frac{t^n}{2\Delta x}\Big(E'((u_k)_{j+1}^n) - E'((u_k)_{j-1}^n)\Big) \right|.$$

We chosed to limit ourselves to 8 Fourier coefficients in (38) for the computations.

4.2. The Mathieu equation revisited

We first simulated the 3-branch entropy solutions by means of (46)-(47). Furthermore, the corresponding intensities have been derived accordingly. The parameters used were $\Delta x = \Delta t = 0.03$ The consistency with the ray-traced solution (30) is clear on Fig.9 despite the fact that u_0 covers a large part of the Brillouin zone. In particular, the parabolic band approach of §3.2 would produce a very poor approximation because $E'(\min(u_0)) = E'(\max(u_0)) = 0$. We consider $V(x) = \cos(x)$ inside (2) with the ansatz (14) where:

$$u_0(x) = \max\Big(0, 0.5\sin(x - \pi/2)\Big), \qquad \mu_0(x) = \frac{1}{\pi}\exp\big(-2(x-\pi)^2\big).$$

However, we also wanted to check the consistency with a direct simulation of (2) by means of (44) with $M = 70$ (*i.e.* 140 Fourier coefficients). On Fig.10, we display the outcome of both approaches for $\Delta t = \Delta x = \varepsilon = 0.02$ for both $T = 0.1$ (before caustic onset) and $T = 1.5$. At this last time, the multivalued solution developed 4 caustics inside the interval $x \in [3, 5.5]$; we observe that in this region, the WKB approximation behaves reasonably well. The WKB ansatz seems to differ significantly from the directly computed Schrödinger solution on the set where $\partial_x\varphi$ vanishes, $\mu \neq 0$; in particular, signals propagate at a correct speed. At last, we show on Fig.11 the decay of the error (45) on the position densities as ε is decreased from 1/10 to 1/65 while holding on $\Delta x = \Delta t = 0.02$. We observe a slow and oscillatory decay, especially outside the Whitham region $x \in [3, 5.5]$. However even in this area, the error (45) remains at a correct level except for the 4 blow-up points. This last feature being an inherent defect of the semiclassical WKB approach; *cf.* [42].

4.3. The discontinuous Kronig-Penney model

We now switch to the potential (19) together with the following initial data:

$$u_0(x) = \max\big(0, 0.5\sin(x)\big), \qquad \mu_0(x) = \frac{1}{\sqrt{\pi}}\exp\Big(-(x-\frac{\pi}{2})^2\Big).$$

Once again, a good agreement is observed between the ray-traced solution (30) and the 3-branch solutions we got out of (46)-(47) after breakup at time $T = 1.3$; see Fig.12. Two differences appear when comparing with Mathieu's equation: stronger oscillations show up on the intensities $\vec{\mu}$ and the (supposedly steady) nonstrict hyperbolicity point $\max(\vec{u})$ isn't well rendered. This is related to the fact that $B \ni \kappa \mapsto E(\kappa)$ varies much more (as can be checked on Fig.8). Thus the effect of numerical viscosity is noticeable; the parameters used were $\Delta x = 0.03$ and $\Delta t = 0.02$. We close this section mentioning that the Fourier scheme (44) extends easily to this case relying on the Fourier decomposition of the considered potential

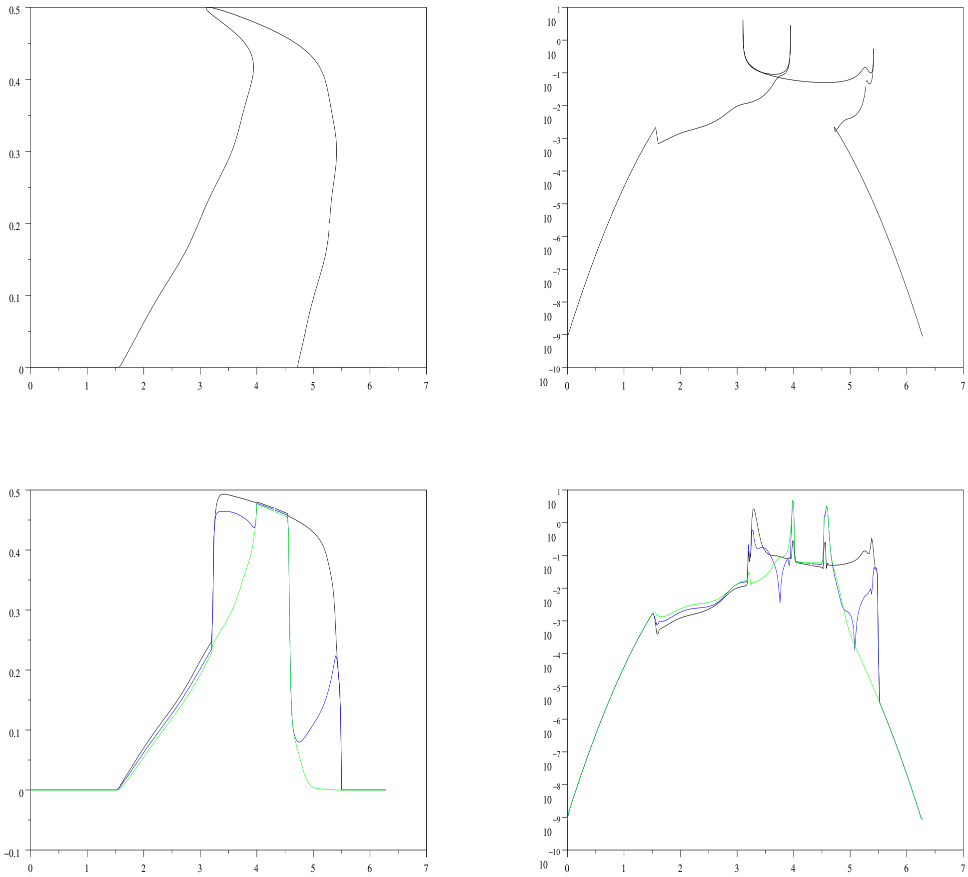

FIG. 9. Exact (top) vs. numerical (bottom) velocities $\vec{u}(1.5,.)$ and intensities $\vec{\mu}(1.5,.)$.

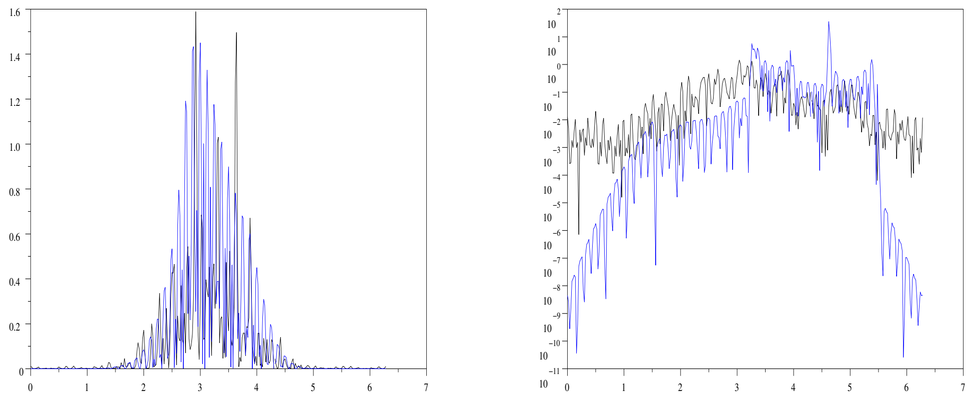

FIG. 10. Densities obtained with Schrödinger and WKB, $\varepsilon = 1/50$; $T = 0.1$ (left), $T = 1.5$ (right).

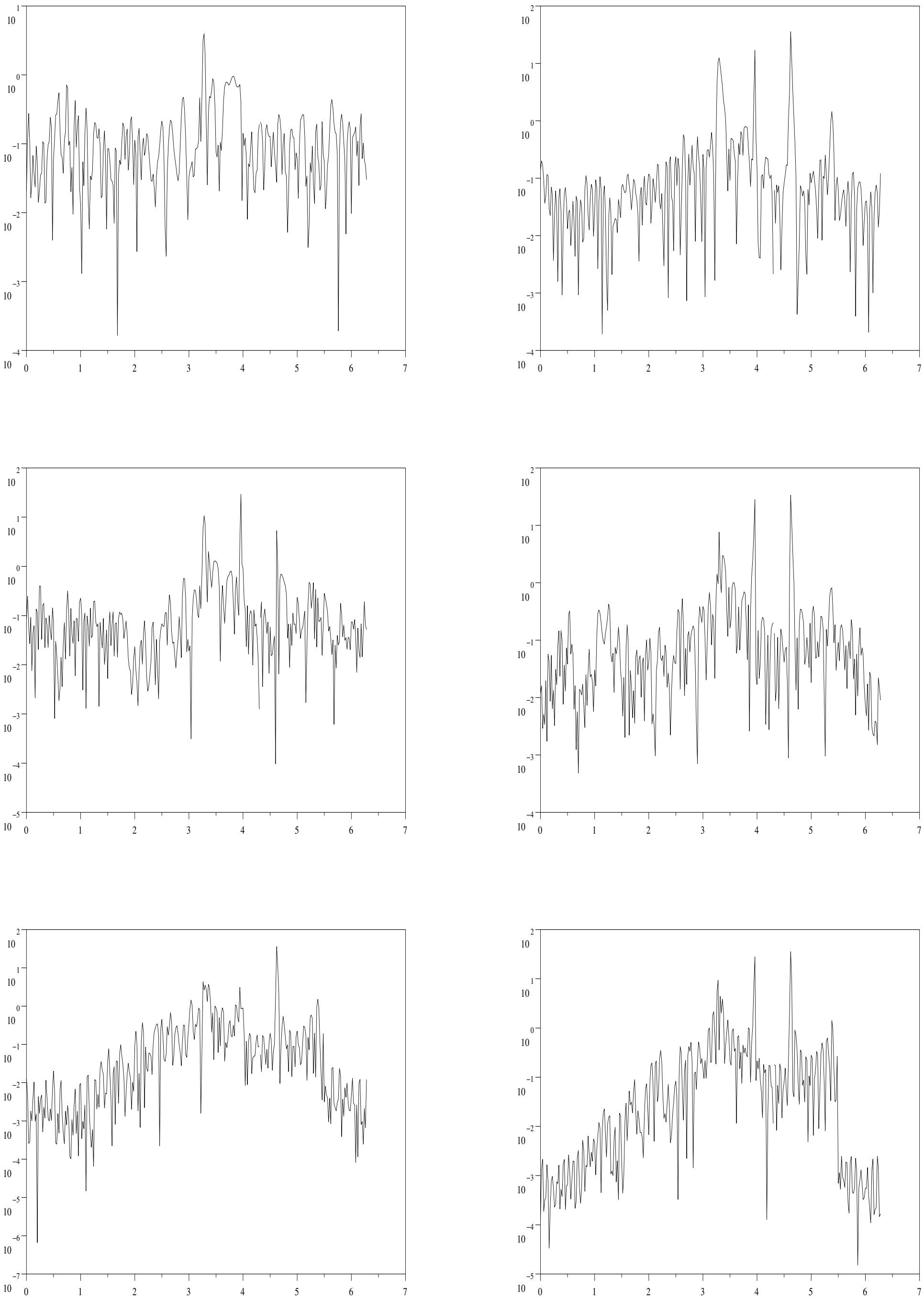

FIG. 11. Errors (45) on the position density with $\varepsilon = 1/10, 1/15$ (first row, left to right), $1/25, 1/35$ (second row), $1/50, 1/65$ (third row) at time $T = 1.5$.

$V(x)$ (which is known to be 2π-periodic):

$$V(x) = \sum_{\ell \in \mathbb{Z}} V_\ell \exp(i\ell x), \qquad V_\ell = \frac{1}{2\pi} \int_0^{2\pi} V(x) \exp(-i\ell x).dx.$$

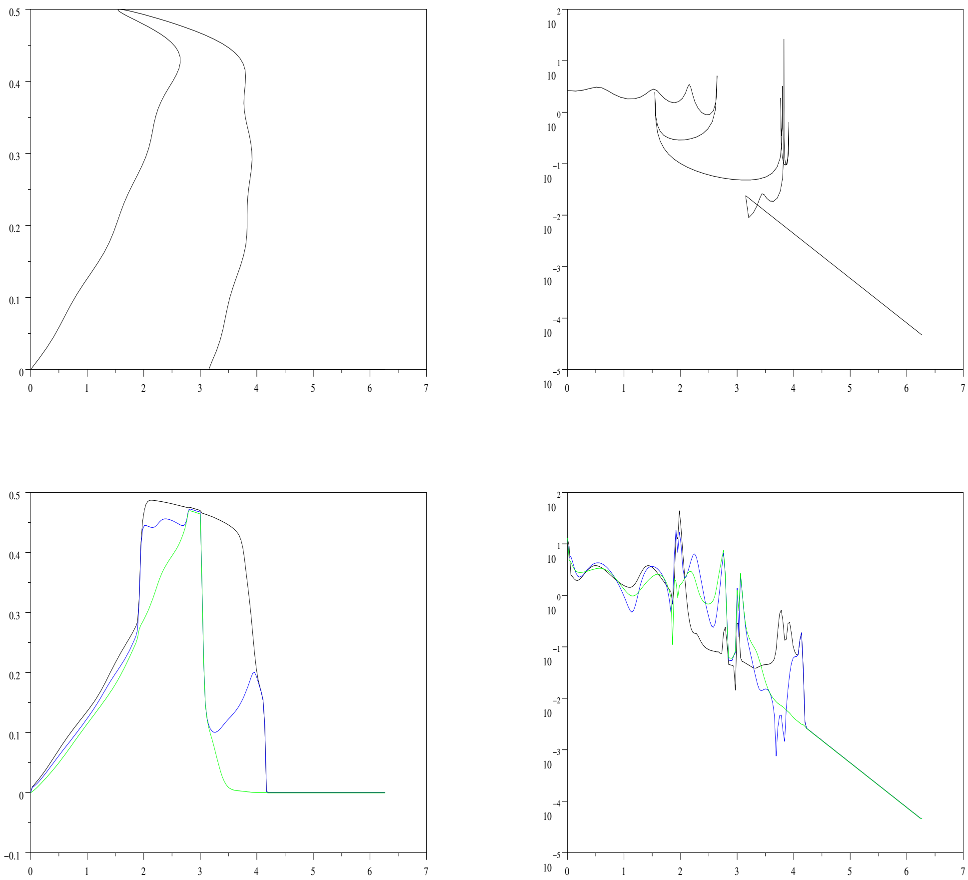

FIG. 12. Exact (top) vs. numerical (bottom) velocities $\vec{u}(1.3, .)$ and intensities $\vec{\mu}(1.3, .)$.

Hence the differential system (44) is modified accordingly for $1/\varepsilon \in \mathbb{N}$:

$$\forall j \in \mathbb{Z}, \qquad i\varepsilon\dot{\psi}_j(t) = \frac{j^2\varepsilon^2}{2}\psi_j(t) + \sum_{\ell\in\mathbb{Z}} V_\ell \psi_{j-\ell/\varepsilon}.$$

Of course, as in §3.2, one can only consider a finite number of Fourier coefficients when integrating this differential system. Actually this enlightens the big difficulty lying in a direct numerical simulation of the semiclassical limit $\varepsilon \to 0$: namely, with smaller ε, the periodic potential affects higher and higher frequencies. The situation gets even worse when low-regularity potentials are involved for which the coefficients V_ℓ do not decay quickly with ℓ.

5. CONCLUSION AND PERSPECTIVES

So far, we have dealt with basic cases where short-scale periodic potentials take into account only for interaction with atoms of identical nature inside the crystal. Now, suppose that we add an impurity from column V in the Periodic Table to a semiconductor such as Silicon or Germanium which are both in column IV. This impurity atom will have one more electron that is needed to satisfy the valency requirements for the tetrahedral bonds formed with 4 electrons. This extra electron will be free to wander through the crystal lattice subject of course to Coulomb attraction of the ion core which will have one unit of positive charge. We are led to consider a slightly more complex Schrödinger equation in place of (1),

$$i\hbar\partial_t\psi + \frac{\hbar^2}{2m}\partial_{xx}\psi = e\left(V(x) - \frac{e}{\epsilon_0|x - x_{donor}|}\right)\psi, \tag{48}$$

and $\epsilon_0 \in [1, 100]$ stands for an average dielectric constant seen by the donor's electron inside the crystal, [3]. Reformulating (48) in atomic units $e = m = \hbar = 1$ ans assuming that V is 2π-periodic on the atomic length scale, the macroscopic scaling is determined by the slowly-varying perturbation,

$$\varepsilon = \frac{1}{\epsilon_0}, \qquad i\varepsilon\partial_t\psi + \frac{\varepsilon^2}{2}\partial_{xx}\psi = \left(V\left(\frac{x}{\varepsilon}\right) - \frac{1}{|x - \varepsilon x_{donor}|}\right)\psi, \tag{49}$$

and one deduces from band Wigner theory, see §2.3 and [3, 23, 31, 44], that the dynamics of (49) are given by the n^{th} band Hamiltonian: $E_n(p) - \frac{1}{|x-\varepsilon x_{donor}|}$. This way, the WKB systems (15) are now endowed with a source term:

$$\partial_t\varphi + E_n(\partial_x\varphi) = \frac{1}{|x - \varepsilon x_{donor}|}; \qquad \partial_t\mu + \partial_x\Big(\mu\ E_n'(\partial_x\varphi)\Big) = 0. \tag{50}$$

Taking x-derivatives, one finds out that $F = E_n$ and $G(x) = -1/|x - \varepsilon x_{donor}|$ in (32). Thus K-branch solutions are to be processed using sophisticate well-balanced techniques as in [26, 27, 29], but in a nonconvex and nonstrictly hyperbolic context. These topics will be developed in the forthcoming Part II of this work.

APPENDIX: NAIVE WKB AND EFFECTIVE HAMILTONIANS

We saw at the beginning of §2 that in the simplest case $V_e \equiv 0$, a naive WKB approach (8) leaves us with

$$\partial_t\varphi^\varepsilon + \frac{1}{2}(\partial_x\varphi^\varepsilon)^2 + V\left(\frac{x}{\varepsilon}\right) = 0,$$

and this Eikonal equation can possibly be homogenized following [38] in order to get rid of the fast scale $y = x/\varepsilon$. By construction $x \mapsto \mathcal{H}(p, x)$ is 2π-periodic and we can seek the limiting behaviour of viscosity solutions φ^ε. Indeed, under mild hypotheses, $\varphi^\varepsilon \to \varphi$ satisfying in the sense of viscosity

$$\partial_t\varphi + \bar{\mathcal{H}}(\partial_x\varphi) = 0, \tag{A.1}$$

where $p \mapsto \bar{\mathcal{H}}(p)$ is the effective Hamiltonian whose derivation goes as follows. One considers the so-called "cell problem",

$$\mathcal{H}(p + \partial_y v(y), y) = \alpha, \qquad (y, p) \in \mathbb{R}^2. \tag{A.2}$$

Then it is proved in [38] that for a given $p \in \mathbb{R}$, there is a unique $\alpha = \alpha(p) \in \mathbb{R}$ such that (A.2) admits a (possibly not unique) 2π-periodic viscosity solution $y \mapsto v(y)$.

Hence the effective Hamiltonian in (A.1) reads:

$$\bar{\mathcal{H}}(p) = \alpha.$$

This has connections with both classical (a so-called "generating function of a canonical transformation" u, [35, 21] is $u(y) = py + v(y)$ when v is smooth) and quantum mechanics. In fact, following [20], we consider the eigenproblem (11) and assume for Ψ:

$$\Psi(y) = \exp(ipy)\phi(y), \qquad \phi(y) = a(y)\exp(iv(y)).$$

Then, from (11), we deduce:

$$\frac{1}{2}|p + \partial_y v(y)|^2 + V(y) = E(p) + \frac{\partial_{yy} a}{2a}, \qquad \partial_y\big(a(y)^2(p + \partial_y v)\big) = 0.$$

This hints that $\bar{\mathcal{H}}(p) = E(p)$ is related to the Bloch spectrum of $\mathcal{H}(y, \hat{p})$ for those bands for which the amplitude variations are small. We can go a bit further for instance considering the particular case $V(y) = \cos(y)$ inside (A.2):

$$v(y) = -py \pm \int_0^y \sqrt{2(\bar{\mathcal{H}}(p) - \cos(s))}.ds, \qquad y \in [0, 2\pi].$$

Two cases occur:

- if $\bar{\mathcal{H}}(p) \geq \max(\cos(y))$, then $v \in C^1_{per}(\mathbb{R})$. A consequence of 2π-periodicity is

$$v(0) = 0 = v(2\pi) \Rightarrow p = \pm\frac{1}{2\pi}\int_0^{2\pi} \sqrt{2(\bar{\mathcal{H}}(p) - \cos(s))}.ds.$$

  And this equation has a solution for $|p| \geq \frac{1}{2\pi}\int_0^{2\pi}\sqrt{2(1-\cos(s))}.ds = \frac{4}{\pi}$.
- if $\bar{\mathcal{H}}(p) < \max(\cos(y))$, then following [38], we take $\bar{\mathcal{H}}(p) \equiv 1 = \max(\cos(x))$.

All in all, this technique gives:

$$\begin{cases} |p| = \dfrac{1}{2\pi}\displaystyle\int_0^{2\pi} \sqrt{2(\bar{\mathcal{H}}(p) - \cos(s))}.ds & \text{for} \quad |p| \geq \dfrac{4}{\pi}, \\ \bar{\mathcal{H}}(p) \equiv 1 = \max(\cos(y)) & \text{for} \quad |p| < \dfrac{4}{\pi}. \end{cases}$$

One recognises some kind of Bohr-Sommerfeld quantization rule which gives flat bands in the non classical regime $E(p) < \max(V(y))$; see [15, 35]. We are displaying $E_1(\kappa)$, $E_2((\kappa - \frac{1}{2}) + 1)$, $E_3(\kappa + 1)$, $E_4((\kappa - \frac{1}{2}) + 2)$, $E_5(\kappa + 2)$ for $\kappa \in [0, \frac{1}{2}]$ in order to compare with $p \mapsto \bar{\mathcal{H}}(p)$. This is inspired by the "nearly free electron model", [3]. When comparing with Fig.4, one notices that for $|\kappa| = \frac{4}{\pi} - 1 \simeq 0.2732$, the first conduction band enters into the classical regime, *i.e.* $E_3(\kappa) > 1$. An illustration is provided within Fig.1.

So, this process isn't well-suited for our program because it would imply for instance an infinite effective mass for the electron since the parabolic band approximation (39) would essentially be:

$$E_3(p) = E_3(0) = 1.$$

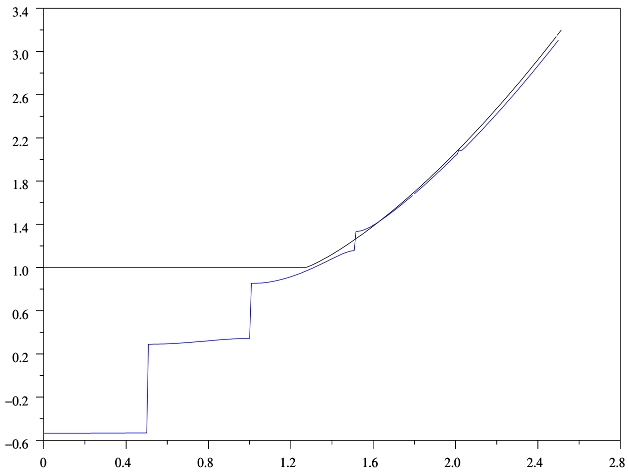

FIG. 1. Comparison between $\bar{\mathcal{H}}(p)$ and the band structure for $V(x) = \cos(x)$.

In the case of the discontinuous Kronig-Penney's model, one obtains a very simple simple formula for $\bar{\mathcal{H}}$:

$$\begin{cases} |p| = \dfrac{1}{2}\left(\sqrt{2\bar{\mathcal{H}}(p)} + \sqrt{2(\bar{\mathcal{H}}(p) - 1)}\right) & \text{for} \quad \bar{\mathcal{H}}(p) \geq 1, \\ \bar{\mathcal{H}}(p) \equiv 1 = \max(V(y)) & \text{otherwise.} \end{cases}$$

See the numerical results on Fig. 2.

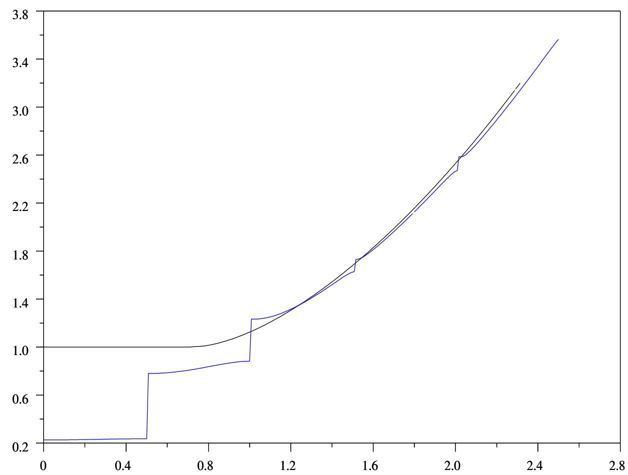

FIG. 2. Comparison between $\bar{\mathcal{H}}(p)$ and the band structure for Kronig-Penney's model.

Acknowledgements. Both authors were partially supported by the EEC network #HPRN-CT-2002-00282 and by the Wittgenstein 2000 Award of P. A. Markowich funded by the Austrian Research Fund FWF. Also support from the Austrian FWF project P14876 Nr.4 is acknowledged.

REFERENCES

1. S. Alinhac, Blowup for nonlinear hyperbolic equations, PNLDE **17**, Birkhäuser Verlag 1995
2. D. Amadori, L. Gosse & G. Guerra, *Global BV entropy solutions and uniqueness for hyperbolic systems of balance laws*, Arch. Rational Mech. Anal. **162** (2002) 327–366.
3. N.W. Ashcroft and N.D. Mermin, Solid-state physics, Holt; Rinehart and Winston 1976.
4. F. Ancona, A. Marson, *A wave front tracking algorithm for $N \times N$ non genuinely nonlinear conservation laws*, J. Differential Equations, **177** (2001), 454–493.
5. J.D. Benamou, *Direct computation of multivalued phase space solutions for Hamilton-Jacobi equations*, Comm. Pure Appl. Math. **52** (1999), 1443 – 1475
6. A. Bensoussan, J.L. Lions, G. Papanicolaou, Asymptotic analysis for periodic structures, Amsterdam; North-Holland 1978.
7. F. Bloch, *Über die Quantenmechanik der Electronen in Kristallgittern*, Z. Phys. **52** (1928) 555-600.
8. F. Bouchut and F. James, *One-dimensional transport equations with discontinuous coefficients*, Nonlinear Analysis TMA, **32** (1998), 891 – 933.
9. F. Bouchut and F. James, *Duality solutions for pressureless gases, monotone conservation laws and uniqueness*, Comm. P.D.E. **24** (1999) 2173–2189.
10. F. Bouchut, S. Jin, X. Li, *Numerical Approximations of Pressureless and Isothermal Gas Dynamics*, SIAM J. Numer. Anal., to appear.
11. Y. Brenier, *Averaged multivalued solutions for scalar conservation laws*, SIAM J. Numer. Anal. **21** (1984), 1013 – 1037.
12. Y. Brenier and L. Corrias, *A kinetic formulation for multibranch entropy solutions of scalar conservation laws*, Ann. I.H.P. Nonlinear Anal. **15** (1998), 169 – 190.
13. Y. Brenier, E. Grenier, *Sticky particles and scalar conservation laws*, SIAM J. Num. Anal. **38** (1998), 2317-2328.
14. M. Christ & A. Kiselev, *WKB and spectral analysis of one-dimensional Schrödinger operators for slowly varying potentials*, Comm. Math. Phys. **218** (2001), 245–262.
15. Y. Colin de Verdiére & B. Parisse, *Singular Bohr-Sommerfeld rules*, Comm. Math. Phys. **205** (1999), 459–500.
16. C. Conca, S. Natesan, M. Vanninathan *Numerical experiments with the Bloch-Floquet approach in homogenization*, preprint.
17. J.N.L. Connor, T. Uzer, R.A. Marcus, *Eigenvalues of the Schrödinger equation for a periodic potential with nonperiodic boundary conditions; a uniform semiclassical analysis*, J. Chem. Phys. **80** 10 (1984) 5095 – 5106.
18. M. Crandall, P.L. Lions, *Viscosity solutions of Hamilton-Jacobi equations*, Trans. Amer. Math. Soc. **282** (1984), 487 – 502.
19. B. Engquist, O. Runborg and A.K. Tornberg, *High frequency wave propagation by the segment projection method*, J. Comp. Phys. **178** (2002) 373–390.
20. L.C. Evans, *Effective Hamiltonians and quantum states*, Séminaire X-EDP 2000–2001; `http://math.polytechnique.fr/seminaires/seminaires-edp/2000-2001/evans.ps`.
21. L.C. Evans and D. Gomes, *Effective Hamiltonians and averaging for Hamiltonian dynamics, I*, Arch. Rational Mech. Anal. **157** (2001), 1–33.
22. E. Fatemi, B. Engquist and S. Osher, *Numerical solution of the high frequency asymptotic expansion for the scalar wave equation*, J. Comp. Physics, **120** (1995), 145-155.
23. P. Gérard, P.A. Markowich, N.J. Mauser, and F. Poupaud. Homogenization limits and Wigner transforms, Comm. Pure Appl. Math. **50** 4 (1997) 323–379.
24. P. Goatin, *Oleinik estimates and uniqueness for hyperbolic systems of balance laws*, Math. Models Meth. Appl. Sci., to appear.

25. P. Goatin & L. Gosse, *Decay of Positive Waves for $n \times n$ Hyperbolic Systems of Balance Laws*, Proc. Amer. Math. Soc., to appear.

26. L. Gosse, *A nonconservative approach for hyperbolic systems of balance laws: the well-balanced schemes*, in "Hyperbolic problems: theory, numerics, computations", H. Freistuhler & G. Warnecke Eds. Birkhaüser Verlag INSM **140** (2002) 453–461.

27. L. Gosse, *Using K-branch entropy solutions for multivalued geometric optics computations*, J. Comp. Phys. **180** (2002) 155–182.

28. L. Gosse & F. James, *Convergence results for an inhomogeneous system arising in various high frequency approximations*, Numer. Math. **90** (2002), 721 – 753

29. L. Gosse, S. Jin and X. Li *Two moment systems for computing multiphase semiclassical limits of the Schrödinger Equation*, Preprint.

30. J.C. Guillot, J. Ralston, E. Trubowitz, *Semiclassical asymptotics in solid-state physics*, Comm. Math. Phys. **116** (1988) 401–415.

31. F. Hövermann, H. Spohn, S. Teufel, *Semiclassical limit for the Schrödinger equation for a short scale periodic potential*, Comm. Math. Phys. **215** (2001) 609–629.

32. S. Izumiya & G.T. Kossioris, *Geometric singularities for solutions of single conservation laws*, Arch. Rational Mech. Anal. **139** (1997) 255 – 290.

33. Shi Jin & X. Li, *Multi-phase computations of the semiclassical limit of the Schrödinger equation and related problems: Whitham vs. Wigner*, Physica D (to appear).

34. Shi Jin & S. Osher, *A level set method for the computation of multivalued solutions to quasilinear hyperbolic PDEs and Hamilton-Jacobi equations*, Preprint (2003).

35. J.B. Keller, *Semiclassical mechanics*, SIAM Review **27** (1985), 485–504.

36. H.J. Korsch, M Glück, *Computing quantum eigenvalues made easy*, Eur. J. Phys. (submitted).

37. R. Kronig and W.G. Penney, *Quantum mechanics of electrons in crystal lattices*, Proc. Royal Soc. A **144** (1931) 101.

38. P.L. Lions, G. Papanicolaou and S.R.S. Varadhan, *Homogenization of Hamilton-Jacobi equations*, unpublished manuscript, circa 1988.

39. P.L. Lions and T. Paul, *Sur les measures de Wigner*, Revista. Mat. Iberoamericana **9** (1993) 553-618.

40. P.L. Lions, B. Perthame, E. Tadmor, *A kinetic formulation of multidimensional scalar conservation laws and related equations*, J. Amer. Math. Soc. **7** (1994), 169 – 191.

41. P.L. Lions, B. Perthame, E. Tadmor, *Kinetic formulation of the isentropic gas dynamics and p-systems*, Comm. Math. Phys. **163** (1994), 415 – 431.

42. D. Ludwig, *Uniform expansions at a caustic*, Comm. Pure Appl. Math., **19** (1966), 215-250.

43. P. Markowich, N.J. Mauser, F. Poupaud, *A Wigner-function approach to semiclassical limits: electrons in a periodic potential*, J. Math. Phys. **35** (1994), 1066–1094.

44. F. Poupaud and C. Ringhofer, *Semi-classical limits in a crystal with external potentials and effective mass theorems*, Comm. Partial Diff. Eq. **21** (1996), 1897–1918.

45. O. Runborg, *Some new results in multiphase geometrical optics*, Math. Mod. Numer. Anal. **34** (2000), 1203 – 1231.

46. C. Sparber, P. Markowich, N. Mauser, *Multivalued geometrical optics: Wigner functions vs. WKB methods*, Asymptotic Anal., to appear.

47. W.W. Symes and J. Qian, *A slowness matching Eulerian method for multivalued solutions of Eikonal equations*, submitted to J. Sci. Comp.

48. A. Vasseur, *Convergence of a semi-discrete kinetic scheme for the system of isentropic gas dynamics with $\gamma = 3$*, Indiana Univ. Math. J. **48** (1999), 347 – 364.

49. A. Vasseur, *Time regularity for the system of isentropic gas dynamics with $\gamma = 3$*, Comm. P.D.E. **24** (1999), 1987 – 1997.

50. A. Zettl, *Spectral theory and computational methods for Sturm-Liouville problems*, in D. Hinton and P.W. Schaefer Eds, Lect. Notes in Pure and Applied Math. **191** (M. Dekker 1997).